Constance Mirror Program: Progress and Plans

by
R. E. Klinkowstein, M. E. Mauel, J. Irby, L. D. Smullin, S. Voldman

March 3,1981
Plasma Fusion Center
Research Laboratory of Electronics
Massachusetts Institute of Technology

Abstract

The basic construction of the Constance II experiment was completed during August of 1979 with the installation of the first set of Ioffe bars. Since then, several improvements have been made and several experimental investigations have been completed. These are: (1) the improved, liquid-nitrogen cooled, Ioffe bars have been constructed and installed, (2) a diverter coil was installed between the guide and mirror field region, (3) the 100kW ICRF generator has been constructed and tested, (4) the data acquisition system has been completed, (5) confinement studies have determined the optimum hot-ion operation of the machine with Titanium and pulsed-gas plasma guns, (6) the density, temperature, and radius of the plasma has been measured, (7) ion-cyclotron fluctuations have been observed, their bandwidth measured, and the conditions for its appearance investigated, and (8) preliminary ECRH data have been collected demonstrating resonance heating. In addition, development of the diagnostics has continued. For example, new x-ray diagnostics have been designed and purchased, and progress on the Thomson scattering has been made. Finally, a new hot cathode gun, which will soon be tested, has been designed and constructed. This report discusses the current state of the mechanics of the Constance II experiment as well as the physics results that have been gathered to date. In addition, the motivation, background, and future plans for the Constance II experiment will be reviewed.

Acknowledgments

The Constance I and II mirror experiment is supported by D.O.E. Contracts DE-AC02-78ET-51013 and No.DE-AS02-78ET-53076. The members of the group are Rose Bella (group secretary), Steve Bradley, Stuart D. Brorson, Robert J. Davco (mechanical technician), Amin K. Ezzeddine, Michael Furuno, Richard C. Garner, Dr. James H. Irby, Dr. Robert E. Klinkowstein, Michael E. Mauel, Kenneth F. Rettman (research technician), Professor Louis D. Smullin (group leader) and Steven H. Voldman. The progress and results so far obtained would not have been possible without the contributions and hard work of all of the group members.

The data acquisition system is implemented with the Plasma Physics TV Display System and the Macsyma Consortium Computer supported in part by the National Aeronautics and Space Administration under grant NSG 1323, by the Office of Naval Research under grant N00014-77-C-0641, by the U. S. Department of Energy under grant ET-78-C-02-4687, and by the U. S. Air Force under grant F49620-79-C-020.

Contents

Summary

This report is a summary of the Constance Mirror Program. The Constance program is guided by mirror physics issues relevant to the National Mirror Program. Specifically, we have concentrated on problems of plasma microstability in minimum-B magnetic geometry associated with endplugs and MHD anchors of the tandem mirror. Until recently,microstability was the central thrust of experimental mirror research. However, with the advent of the tandem mirror and its successful demonstration in TMX, many new ideas and issues have competed for the attention of the experimental plasma physics community. Obtaining microstability in a mirror confined plasma remains an important issue and one which will ultimately affect the success of the tandem mirror. Within the context of microstability, new problems and questions continue to evolve. For example, the stability of sloshing ion distributions and plugs with thermal barriers generated by groups of heated electrons. These types of physics issues determine the role that the Constance program plays in the mirror program. In addition, we are continually assessing the ability of the Constance II experiment to address other areas of mirror research. In particular, problems of electron heating are ideally suited to capabilities of Constance II, and in this report we outline an ECRH program to address many relevant heating questions.

This report is organized into six chapters. The first chapter gives a summary of the experimental results of the Constance program and a background and motivation for each of the four areas of mirror research currently being pursued. These areas are; 1) Hot electron stabilization of microinstabilities, 2) Electron cyclotron heating, 3) Ion cyclotron heating, and 4) Plasma gun studies. The second chapter gives an up to date report on the construction and mechanical status of Constance II. Several important changes have been made and new diagnostics installed during the past year. These are discussed in Chapter 2. Chapter 3 presents data from the confinement studies we have made and describes the plasma parameter regime available to us on Constance II. The final three chapters describe the objectives and status of the experiments performed thus far in our ICRF, ECRH, and plasma gun programs respectively.

The Constance II experiment is a minimum B mirror device fueled by a hydrogen loaded titanium washer gun. Its design parameters were chosen to make it suitable for studying microinstabilities driven by the ion loss-cone distribution inherent to a population of mirror confined ions. In addition its modest size and simplicity permit a diverse program of mirror physics issues to be addressed.

The basic construction of the Constance II experiment was completed by September 1979 with the installation of the first set of quadrupole Ioffe bar coils. Since then, several improvements have been made, several experimental investigations have been completed, and our diagnostic capabilities have grown considerably. The major improvements and additions to the experiment have been; (1) an improved liquid nitrogen cooled Ioffe bar design allowing better diagnostics access and significantly improved neutral gas control; (2) a 100kW ICRF generator; (3) a diverter coil located between the mirror and guide fields; (4) a data acquisition system interfaced to the M.I.T. Macsyma Consortium Computer; and (5) A Thomson scattering system is being built and will be completed by June 1980. Thus far we have completed experiments to determine the optimum operation of Constance II for producing hot ion plasmas using titanium and gas puffed washer guns. In addition, we have have measured density profiles, electron temperatures, and characterized an instability that is observed during the decay of a hot ion plasma. Finally, we have performed preliminary ICRF and ECRH heating experiments.

The operation of Constance II is characterized by two distinct operating modes. For relatively short injection times, which result in line densities of $\lesssim 10^{12} cm^{-2}$, a hot ion, mirror trapped plasma is produced. This plasma exhibits confinement times which are characteristic of the expected collisional and drag processes. Under the proper vacuum conditions, this low density, high ion temperature ($T_i \simeq 150eV$) plasma exhibits an instability at the ion cyclotron frequency. The other mode of operation produces substantially higher densities ($nl \lesssim 5 \times 10^{13} cm^{-2}$), but the plasma is characterized by a two temperature ion distribution, a cold ion component, and a hot ion component ($T_i \sim 150eV$). The density of the hot component is always $\lesssim 10^{12} cm^{-3}$. For these long injection, high density discharges, ion cyclotron fluctuations are never observed. We believe that this upper density limit of hot ion is associated with the plasma gun operation, and we have therefore undertaken a program to study the titanium washer gun and modified washer gun designs which utilize a puffed gas valve for the source of hydrogen. This program has yielded gun designs better capable of controlling the plasma density, but higher hot-ion densities $> 10^{12} cm^{-3}$ have not been produced. In addition, we are nearing completion of a hot cathode plasma gun similar in design to the plasma source used by Ioffe *et al*, [Ref.17]. This gun has been used to successfully produce plasmas in the range $T_i \simeq 150eV$, $ni \lesssim 3 \times 10^{13} cm^{-2}$ on the PR-6 and PR-7 experiments.

An ICRF heating program has also been undertaken to increase the density and temperature of the trapped ions in Constance II. A 100kW, 5 MHz transmitter was constructed with surplus parts. Utilizing this transmitter with a two turn loop antenna we have successfully raised the ion temperature to 460eV at a power level of 50kW. We have also demonstrated an enhanced trapping of the gun injected plasma. Thus far, the application of ICRF heating to the Constance II plasma has not enhanced the observed instability, however, the results are preliminary. We plan to continue this program of ICRF heating with the objective of evaluating the microstability of ICRF heated plasmas.

The hot electron stabilization studies begun on PR-6 (Ioffe,*et al.*, [Ref.17]) and Constance I is continuing on Constance II. The first stabilization experiments have already been conducted with ECRH during unstable, low density discharges. Future work will compare the electron beam and the ECRH techniques of making hot electrons.

Finally, preliminary results of the ECRH program are reported. Good absorption is observed for the extraordinary wave heating used for the experiments. Net heating efficiencies of 30% were measured. Heating has been observed at the first and second harmonics. No high density cutoff has been observed, although this may be due to edge heating. Measurements of the bulk electron temperature with a Langmuir probe and of the total energy with a diamagnetic loop indicate the same "type" of heating observed in Constance I. The bulk electron temperature rises by about a factor of 3-5 and a new ($\sim$ 10 to 20%) population of warm, 300-600eV, electrons is formed. The warm electrons appear to make up the largest proportion of the observed energy rise. Future experiments will include Thomson scattering and soft and hard x-ray diagnostics. We plan detailed measurements of the evolution of the electron energy distribution for several heating geometries pertinent to the tandem mirror program.

8

Introduction

1. Hot Electron Stabilization .

The most important physics issue of tandem mirrors is the microstability of the endplugs [Ref.3]. These microinstabilities are referred to as the drift-cyclotron-loss-cone (DCLC), Alfven-loss-cone (ALC), and negative energy wave (NEW) instabilities of which only DCLC has been observed experimentally [Ref. 7]. As evidenced by high beam-current operation in TMX, the presence of the DCLC instability enhances central cell losses and severely reduces endplug ion-confinement [Ref. 44]. To insure high efficiency, future reactors must maintain microstability of the endplugs.

Fortunately, with the use of outboard, A-cell barriers, the electrostatically confined central-cell ions can fill the low energy, ambipolar hole of the hotter, endplug-ions. Recent theory has shown that, if the barriers work as planned, this overlap of the central-cell ions into the plug region will stabilize all plug microinstabilities in TMX-upgrade and MFTF-B [Refs. 29,31].

However, other tandem mirrors issues such as the effects of MHD ballooning modes and central-cell, drift-resonance transport, have not yet been resolved. Future designers may be faced with the unpleasant choice of micro-unstable endplugs with good radial confinement or microstable endplugs with poor radial confinement. For example, TARA, the proposed tandem mirror at M.I.T., has two outboard anchors with an axisymmetric barrier cell [Ref. 45]. In this case, the axisymmetric drifts of the central cell ions eliminates resonance transport, but the outboard anchor is bare of the overlapping central-cell ions and must be stabilized by some other means.

The search for an efficient and reliable alternate means of DCLC stabilization motivates the Constance II hot electron stabilization experiments.

Stream stabilization, hot electron stabilization, and the stabilization due to electrostatically confined ions in a sloshing-ion plug are the only alternate techniques suggested at this time. Stream stabilization, which is reasonably well understood, refers to the forced filling of the ion's ambipolar hole by injection of a warm "stream" from a plasma gun or a gas box. Stream stabilization was successful in stabilizing 2XIIB but the stream cooled the electrons and significantly reduced the ion confinement due to electron drag. On the other hand, hot electron stabilization has the bonus of heating the electrons during stabilization. Ioffe and Kanaev [Ref. 18,19] first demonstrated this technique by creating with ECRH a disk of magnetically confined electron in the mirror midplane. The experimental results have been well explained experimentally

by the argument that the electrons depress the midplane potential and electrostatically trap a sufficient population of cool ions to fill the ambipolar hole [Ref. 19].

The PR-6 experiments lead to the only other successful, hot electron stabilization experiments. These were the Constance I E-beam stabilization experiments conducted by Klinkowstein and Smullin [Ref. 22], and, later, the Constance I ECRH experiments [Ref. 25]. Both the Soviet and Constance I experiments observed enhancement of the instability at low to moderate powers and stabilization at higher powers. The first effect was attributed to bulk electron heating which widened the ambipolar hole, and the second to the accumulation of sufficient hot electrons to somehow cause stabilization. In addition, the increase in diamagnetism during the onset of stabilization was remarkably similar for all three experiments. However, an important difference between both the E-beam and ECRH experiments of Constance I and those of PR-6 is the large axial spread in the electron distribution found in Constance I as compared with the localization to the mirror midplane of the hot electrons in PR-6. This suggests that other mechanisms like ∇B-drift damping and electron Landau damping may also contribute to the process of hot electron stabilization in addition to the confinement of cool ions in local potential depressions.

The Constance II experiment was designed for the purpose of diagnosing the mechanism and scaling of the hot electron stabilization observed in Constance I. The better diagnostics and vacuum access provide an improved test stand for the investigations of hot electron stabilization. In addition, E-beam stabilization can be compared with ECRH stabilization under identical conditions and diagnostics. However, as will be described in the section on confinement studies, the Constance II plasma is unstable to ion cyclotron fluctuations only for densities less than $10^{12} cm^{-3}$. This is probably due to the observed decrease in hot ion production as plasma density increases. Since this restricts the range of densities over which the electron heating can be shown to stabilize the instability, the ability to determine the usefulness of the technique for higher density tandem mirrors is limited. Consequently, new plasma guns have and are being constructed which may increase the density at which DCLC and hot ions are observed. This is discussed further in the section on plasma gun studies.

Finally, the other scheme to stabilize DCLC is by use of a sloshing-ion distribution [Ref. 21]. Here, the bulk of the ions have turning points near the mirror peaks which creates a density and potential depression at the mirror midplane. This is exactly the same idea behind the stabilization observed in PR-6 except, in this case, hot ions are excluded from the midplane instead of cold electrons. This method of stabilization may also be tested in Constance II by tuning the ICRF to be resonant off-axis. This is explained further in the section on ICRF heating.

2. ECRH Program

Current plans for tandem-mirror-reactors require electron-cyclotron heating to maintain the high potentials of the endplugs [Ref. 5]. Plug electrons are heated to energies several times higher than the average central-cell electron energy and thermal barriers [Ref. 2] slow the heat exchange between the two electron populations. The addition of thermal barriers and electron heating to TMR designs reduce the

projected plug input power by a factor of four and simplify plug technology [Refs. 5 and 23]. The 1.2 MeV neutral beams required to maintain a high plug density without barriers can be replaced by the (hopefully more feasible) 100MW collection of gyrotrons. The thermal barrier allows high electron temperatures at low input powers, and the locally high electron temperatures generate high potentials at low densities. The prospect for the improvement of tandem mirrors by the addition of electron heating and barriers has made ECRH a vital and probably an absolutely necessary element in the ultimate success of the tandem mirror reactor.

However, the application of ECRH to dense ($\omega_{pe} \gtrsim \omega_{ce}$), hot-ion mirror-confined plasma is new, and the experimental experience for heating under these conditions is limited.

Most of the past experiments have been ECRH discharges. Of these, the most notable is the extensive work of the scientists at Oak Ridge under the leadership of R. Dandle which lead to the development of EBT [Ref. 9,10]. Other discharges were studied by Fessenden and Smullin [Ref. 12] and Ikegami at Nagoya (Ikegami, [Ref. 15,16]). Also, one of the only minimum-$|B|$ discharges was the INTERM experiment [Ref. 14]. The ECRH discharge differs from the heating of hot, highly-ionized plasmas since (1) the discharge is created from microwave-ionization of the high neutral gas, (2) most of the RF energy was absorbed by a superthermal electron-tail, which can develop energies up to several hundred KeV. The hot-tails were well separated energetically from the colder and denser, bulk electrons whose density and temperature was determined by the neutral pressure, the magnetic field, and the drag-power from the hot tail. For high enough pressures, the hot-electron plasmas were stable and built up densities such that $\omega_{pe} \lesssim \omega_{ce}$. Since these plasmas were predominately steady state, and since the hot electrons dominated the power absorption, bulk electron heating and electron energy development have not been studied experimentally in discharges.

For tandem mirrors, the behavior and problems of electron heating of dense "reactor-like" endplugs are expected to be different from that of the old discharge experiments. This is because tandem mirrors will require the "controlled development" of the electron energy distributions. On the one hand, the bulk electrons must be locally heated to raise the positive confining potential of the plugs; while, on the other hand, the barrier electrons must be tail heated to depress the potential and insulate the plug from the central cell. Furthermore, to be efficient, the bulk-heating must guard against the added power drain due to tail-heating. And, in the barrier, the ECRH must be designed to avoid "hot-tail runaway" which would reduce barrier density and, consequently, the barrier's ability to insulate [Ref. 40]. The establishment, time-development, and power balance of a tandem-mirror, ECRH equilibrium has yet to be experimentally studied, theoretically predicted, or understood. In addition, because of the higher densities and temperatures of the modern mirrors, the power absorption, accessibility and refraction of the microwaves has become a much more critical issue in TM's than in ECRH discharges. For example, certain launch angles will enable complete first pass absorption; whereas, slightly different launch angles will allow the microwaves to pass through or bounce around the plasma and heat unwanted resonance zones [Ref. 36].

The few non-discharge experiments that have been constructed to date are characterized by high density ($\omega_{pe} \gtrsim \omega_{ce}$) plasmas formed by plasma guns with low to moderate initial electron temperatures

($T_e \lesssim 20eV$). These include Ioffe and Kanaev with PR-6 [Ref. 19]. Mauel with Constance I and II [Refs. 25 and 26], and, recently, Smatlak [Ref. 41] studying second harmonic heating of Phaedrus. Two important results of the Constance I experiment were the inverse density scaling of hot-electron tail production and the observation of a hot electron instability during high heating powers and low densities.

The first full test of ECRH on tandem mirrors is planned for the TMX-upgrade experiment early in 1982 [Ref. 42]. Here, the hot-electron barrier will be formed with second-harmonic ECRH in large mirror-ratios (R=4), quadrupole-stabilized, sloshing-ion endplugs. First-harmonic heating of the outboard half of the plugs will form the confining potential for the central cell. Other experiments will test variations of this configuration. Tara at MIT will hopefully be in operation late in 1983. Tara will feature an outboard anchor and an axisymmetric plug [Ref. 45]. MFTF-B will have two inbound anchors and the barrier and plug in the outboard A-cells [Ref. 3].

All three of these devices share the idea of using hot, magnetically confined electrons for a barrier (and/or for an MHD anchor) and ECRH to maintain the high plug-cell temperature difference. Unfortunately, ECRH has not been experimentally tested for these applications. Consequently, the tandem mirror experiments will be confronted with two, somewhat overlapping physics tasks: (1) the study of tandem mirror confinement (eg. microstability, radial transport, and potential confinement), and (2) the study of electron cyclotron heating of mirrors.

The Constance II ECRH experiments are designed to help bring timely answers to some of the questions contained in the second task. Although the size, density, and temperature of the Constance II plasma are lower than those expected in TARA and TMX-U, immediate solutions to the mysteries of accessibility, heating rates, ECRH-maintained equilibria, and bulk vs. tail heating would most certainly speed the application of ECRH to future machines. Currently, Constance II is equipped to investigate the following problems:

1. Demonstration and evaluation of the bulk heating of dense, mirror-confined plasmas.

2. The study of the conditions which produce bulk or tail heating and of those producing "ECRH runaway".

3. Formulation of a consistent theory which predicts the observed heating rates and the scaling of the heating with density and temperatures.

In addition, at a later date, Constance II can:

4. Create and evaluate a hot electron barrier by maintaining a localized population of magnetically trapped electrons.

5. And, identify the hot electron instability, and determine the conditions for destabilization.

The procedure and description of the experiments designed to accomplish this are described with more detail in the section on the ECRH program. Also, preliminary results of the ECRH experiments are presented.

3. Ion Cyclotron Heating .

During the past year we have begun to investigate ICRF heating in the Constance II experiment. The goals of the ICRF program are

1. To better control the trapped plasma parameters in Constance II..

2. To investigate the microstability of ICRF heated plasmas.

3. To explore the possibility of producing a sloshing ion distribution using ICRF with stream filling of a mirror.

An ICRF transmitter capable of delivering 100 kW at 5 MHz was constructed in the summer of 1980 from surplus parts. The primary motivation for constructing this transmitter was to increase the ion energy and density of the Constance II plasma. This increase in ion energy would allow us to study plasmas that are potentially more unstable to microinstabilities driven by ion loss-cone distributions. Very little control of the ion temperature is possible with the normal titanium washer gun operation. We hope to be able to control T_i over a range from 150eV - 1keV. In addition to changing T_i, the application of ion cyclotron heating should trap streaming plasma from the washer gun more effectively. The washer gun produced plasma has been shown to be composed of a hot ion component and a cold ion component (see Chapter 3). Thus far we have not been able to produce high density plasmas without a substantial fraction of cold ions. We are hopeful that the application of ICRF can be used to heat the cold component sufficiently to prevent it from stabilizing the ion cyclotron instabilities we study.

The use of ICRF heating as a stabilizing technique to microinstabilities was originally suggested by Kesner [Ref. 21]. The ion distribution function resulting from ICRF heating combined with fueling near the velocity space loss boundary tends to produce a distribution that satisfies $\partial f/\partial E < 0$ throughout most of velocity space, in constrast to neutral beam fueled plasmas. In addition, the ion distribution can be changed by moving the resonance zone between mirror midplane and the mirror peak. We hope to fully explore the microstability of these ICRF heated plasmas.

The use of sloshing ion distributions in quadrupole and axisymmetric endplugs to produce thermal barriers and create microstable MHD anchors, is a current topic of great interest in mirror research. We

plan to investigate the possibility of creating a sloshing ion distribution in Constance II using ICRF heating. By tuning the heating to a resonance far off the mirror midplane and fueling the mirror with a stream gun it may be possible to create a sloshing ion distribution. We are writing a Monte Carlo code to assess the feasibility of producing sloshing ions in Constance II. We plan to measure $f_{ion}(\Theta, E)$ by modifying our charge exchange analyzer to view the plasma at angles of $< 90^{\circ}$ to the magnetic field. If we are successful in producing a density distribution peaked off the mirror midplane we plan to evaluate its confinement properties (i.e. τ_{conf}, stability) and combine our ECR heating to produce a thermal barrier at the midplane.

4. Plasma Gun Studies .

In the Constance experiments, the mirror is loaded with plasma produced in a plasma gun. In our experiments, so far, these have been washer-guns either fueled by an H_2 loaded Ti anode or by a fast gas valve. It is a fortunate fact that these guns produce a plasma with a significant hot ion component, and that the plasma is highly ionized. Thus it is possible to produce a plasma useful for studying mirror problems, with rather simple equipment. However, we have only a limited ability to vary (increase) the ion temperature above $\sim$ 150eV, since the only variables are the gun discharge current and the injected gas.

As part of our overall program, we are studying the plasma streams from the washer guns (Ti and pulsed gas), and we are building a hot cathode (LaB_6) plasma gun for similar studies.

Although we have collected considerable empirical data, we still have no coherent description of the ion heating mechanism. The electrostatic fluctuation spectrum has a strong band in the UHF region $0.2 \lesssim f \lesssim 1.5GHz$. This corresponds roughly to f_{pi}. Although we have searched carefully, we have found no evidence of electron-plasma, f_{p_e}, oscillations, after the first few microseconds of the discharge. Corresponding to the observed density, these should lie in the range of 10-40 GHz.

Future work will continue to focus on the ion heating mechanism, as well as on the study of the hot cathode plasma gun.

Construction and Mechanical Status

1. Vacuum System .

A schematic drawing of Constance II is shown in Figure 2.1. and a photograph of the device as of June 1980 is shown in Figure 2.2. During F.Y.80 the basic device fabrication as outlined in the proposal was completed with the exception of the Thomson scattering equipment. Several new diagnostics were constructed and a new Ioffe bar design was fabricated and installed.

The vacuum system utilizes Ti gettered surfaces throughout to attain the base pressure of 5×10^{-9} Torr. All gettered surfaces are at room temperature with the exception of the Ioffe bar magnet which is at LN_2 temperature. A diverter coil has been installed between the mirror peak and the plasma gun to prevent cold plasma in the guide field region from entering the mirror during the plasma decay period. The diverter coil is energized by an ignitron switched capacitor. The diverter field has a rise time of $50\mu sec$ and decays with a time constant of $600\mu sec$.

A new LN_2 cooled Ioffe bar coil set was installed to improve vacuum condition during plasma injection, and to improve diagnostic access in the mirror region. During the initial operation of Constance II, we discovered that the support structure for the original Ioffe bars intercepted plasma flowing from the plasma gun. In addition, vacuum leaks were discovered in the stainless steel casing of the coil. Subsequently, a new design was fabricated which incorporated LN_2 cooling and a simpler support structure. The LN_2 cooling enabled us to use smaller copper conductors, hence increasing access and providing cooling for the gettered surfaces of the Ioffe bar structure. Figure 2.3 compares the cross sections of the two Ioffe bar designs.

2. Diagnostics .

Several diagnostics have been installed on Constance II during the past year. Listed below is a brief description of each diagnostic and their status of construction or operation.

2.a. Microwave Interferometer . A 60 GHz interferometer is installed at the mirror midplane. Line densities $10^{12}cm^{-2} > nl > 5 \times 10^{13}cm^{-2}$ are routinely measured. The cutoff density is $4.4 \times 10^{13}cm^{-3}$.

2.b. Charge Exchange Analyzer . A three channel charge exchange analyzer is mounted to view the mirror midplane. The analyzer utilizes electrostatic deflection and channeltron detectors. Oxygen is used as

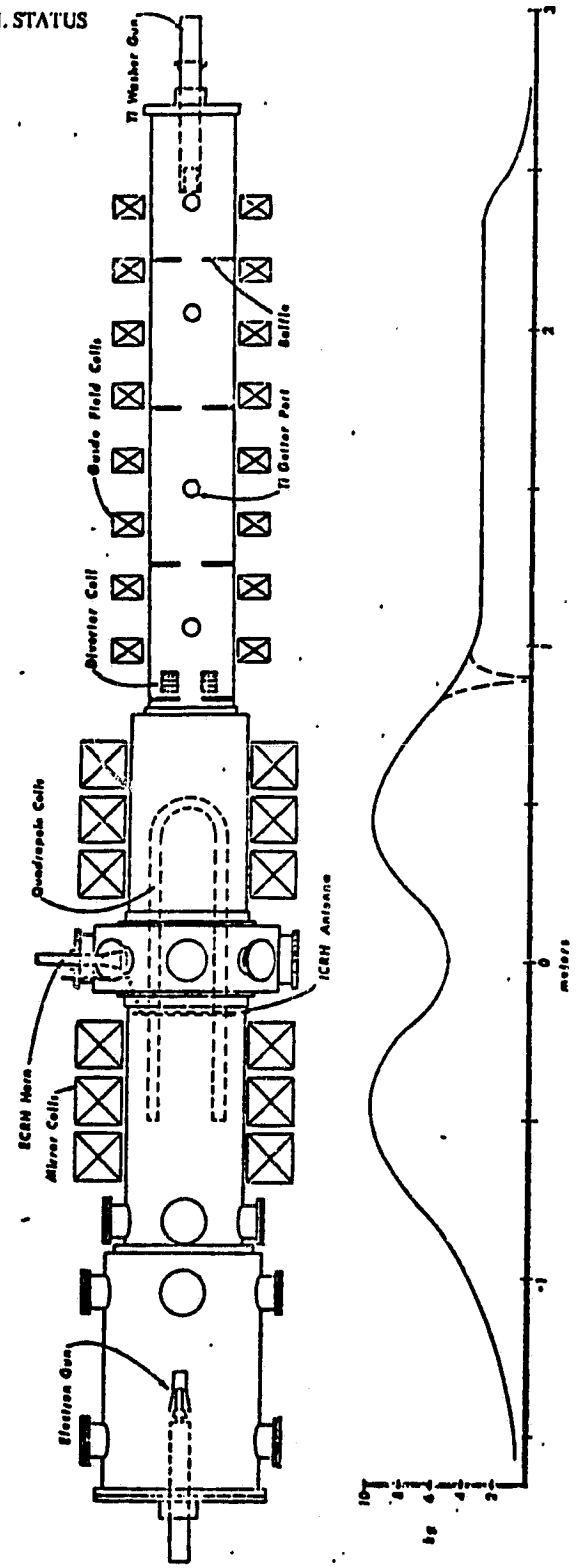

Figure 2.1. A schematic drawing of Constance II

PFC/RR-81-3 MASTER #3002 DOE/ET/51013-5 UC20

Constance Mirror Program: Progress and Plans

by

R.E. Klinkowstein, M.E. Mauel, J. Irby,
L.D. Smullin, S. Voldman

Plasma Fusion Center
Research Laboratory of Electronics
Massachusetts Institute of Technology

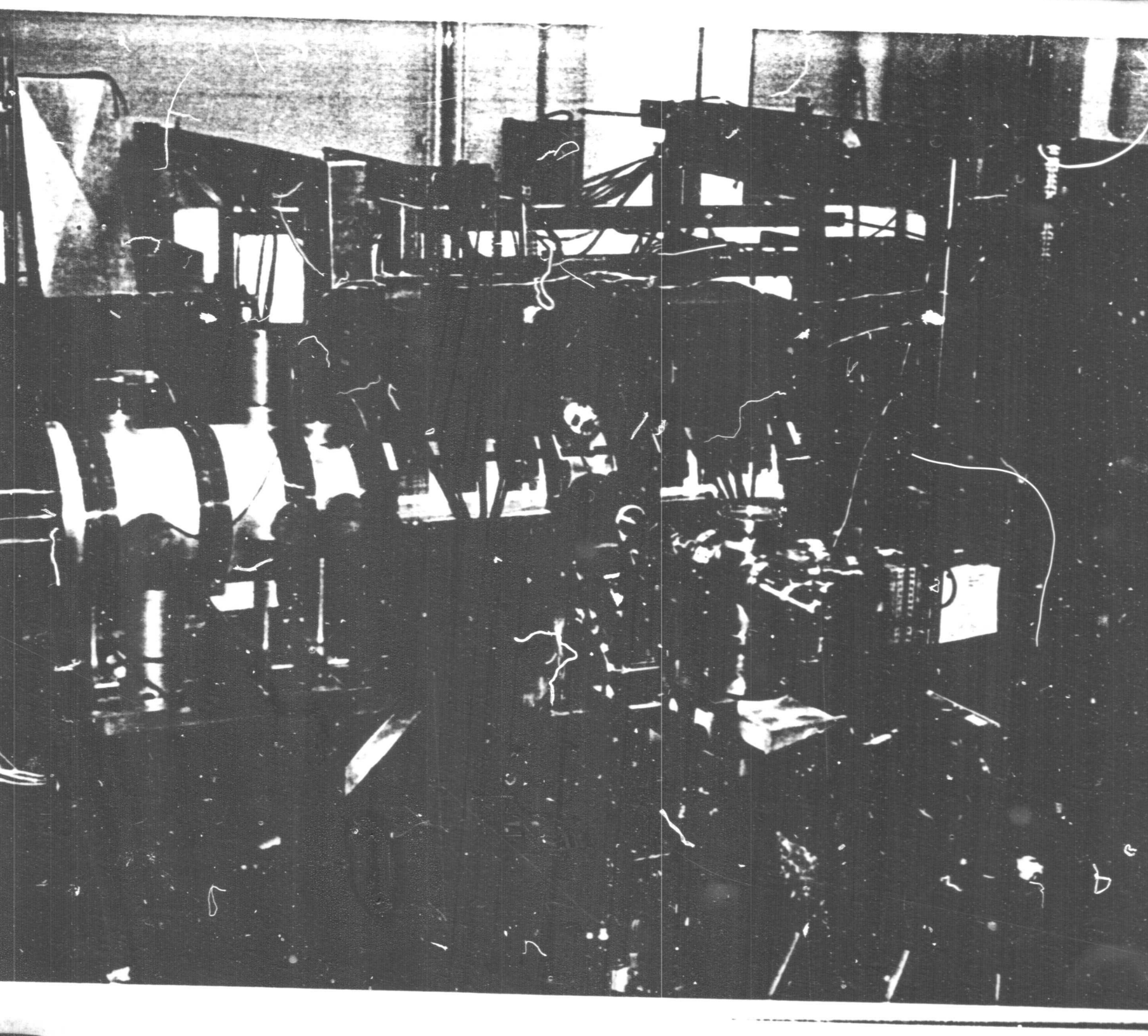

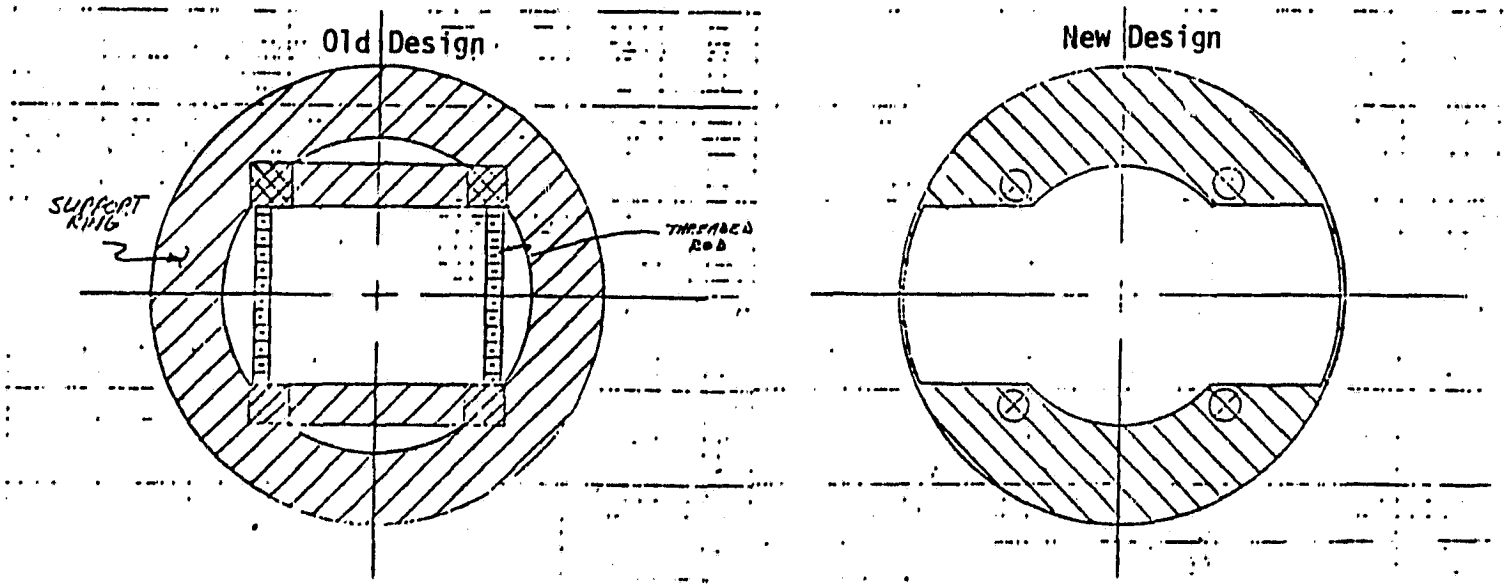

Figure 2.3. A comparison of the old and new Ioffe bar cross sections.

a stripping gas because of the increase in sensitivity it provides for energies below 1 KeV. Ion temperatures have been measured in the range $100eV < T_i < 500eV$. The cross sections for the stripping and CX reactions have been programmed in the computer which enables nearly instant interpretation of the data.

2.c. Probes .

Floating potential probes are used to observe electrostatic fluctuations characteristic of ion cyclotron instabilities. In addition, they are used to measure the low frequency (steady state) value of the floating potential. Two probes are currently mounted in Constance II. A double tip probe is mounted at the mirror midplane and is movable in radius. The probe can be rotated to measure $k \parallel$, $k\perp$. A second probe is movable along the axis and adjustable in radius. In addition, a Langmuir probe mounted at the mirror midplane has been used to measure electron temperature, and density as functions of radius and time. The probe bias voltage can be swept 600 volts in $7\mu sec$.

2.d. Diamagnetic Loop . A 100 turn, electrostatically shielded, diamagnetic loop is mounted 2 cm off the midplane. The loop has been calibrated using two coils to simulate the diamagnetic moment of the plasma. Integration of the loop signal is performed with the aid of our diagnostic computer interface. The loop provides good quantitative data when the machine is operated in a simple mirror (no Ioffe bar field) mode. However, the pulsed nature of Ioffe bar current has made it difficult to obtain reproducible results while

energizing the coil. We have ordered parts for the modification of the Ioffe bar capacitor bank to produce a flat top current for $> 50msec$.

2.e. Spectroscopy . Three spectroscopic instruments have been used on Constance II over the past year. First of all, a .5 meter visible monochromator was used to view the 1/2" plasma gun directly while monitoring various metal impurity lines (mainly titanium). This experiment gave us insight into the metal impurity production rate of the gun. Doppler broadening measurements of H_β line were also made indicating the production of relatively cold hydrogen neutrals by the gun. Secondly, a .2 meter VUV monochromator fitted with a channeltron detector and counting circuit has recently been installed on Constance II. The monochromator has been used to investigate impurity radiation in the vacuum ultraviolet, and to verify the electron temperature measurements of the Langmuir probe. Backfilling of the machine with various impurity gases was used as a calibration of various impurity lines. Preliminary results showed oxygen impurity levels of 5% and somewhat higher impurity levels of carbon. Finally, in a general survey of VUV impurity lines, we found measurable signals from CII, CIV, NIII, OII-OVI, TiII, TiIV, and CuII.

Completing our spectroscopic diagnostics was an Optical-Multichannel-Analyzer (OMA) loaned to us by Princeton Applied Research. With this instrument we were able to judge rather quickly the difference in titanius production between our standard 1/2" plasma gun and a new pulsed gas gun (considerably less for the pulsed gas gun).

2.f. Thomson Scattering . Construction of a Thomson scattering system is nearing completion for installation on Constance II. The entire system has been designed to translate on one optical table, allowing easy alignment and radial measurements. In-line collimation and beam expansion assures a very low divergence, spacially pure beam is focused to a 1 mm spot size within the chamber. The polychromator is a three grating device providing twelve orders of magnitude attenuation of the 6943Å stray light signal. The dispersion is such that reliable measurements should be possible over the range $5 < Te < 100eV$. Six 20Å wide channels detected by Varian VPM 192 photomultiplier tubes feed into a twelve channel charge integrating digitizer. The digitizer interfaces directly to our data acquisition computer.

2.g. Data Acquisition System . Nearly all of the Constance II data are digitized, stored, and processed by a data acquisition system. The system consists of a CAMAC crate, with it's interface and digitizer, connected to the Plasma Physics TV display system and the Macsyma Consortium computer. After each shot, the data are cataloged, processed, and plotted within one and one half minutes.

Two, eight channel 400KHz digitizers are used for the slowly varying signals such as the density, diamagnetism, CX, and soft x-ray signals. Four fast, 20 MHz digitizers allow processing of DCLC fluctuations and fast-sweeping Langmuir probe currents. Interleaving the clocks on the fast digitizer enables FFT analysis up to 20 MHz for $50\mu sec$ intervals. In addition, 3 items have been recently purchased which will expand the data handling capability. The data from the eight hard x-ray channels will be digitized in a scaler; the Thomson scattering data will be recorded by a 12 channel charge digitizer; and a 32 channel ADC

will be used to record various charging voltages and settings before each shot.

2.h. Soft X-Ray Detectors . Soft x-rays of energies between 250eV and 10keV are measured with four ORTEC Series R surface barrier detectors. Beryllium filters are used to select four energy bands within which the radiated bremsstrahlung intensity is measured. Transimpedance preamplifiers have been built for the detectors; currents of $\lesssim 10^{-9}$ amp can be measured at bandwidths of 200 kHz. This equipment will be used primarily to determine the amount of bulk and tail heating resulting from ECR and H^+-beam heating. The surface barrier array is inside the vacuum system and can be tilted radially and axially to help determine the location of the hot electrons.

2.i. Hard X-Ray Diagnostics . The hard x-rays produced from hot electrons from 5 KeV to 50 KeV will be measured by counting scintillation in a fast, Koch-Light, plastic scintillater. The pulses from an RCA 8575 PMT are fed into an eight channel 100 MHz discriminator which will give an indication of the hot electron energy distribution. The output of the discriminator is counted in a 24 bit CAMAC scaler which will be processed by the computer.

2.j. Endloss Analyzer . A five-grid energy analyzer has been installed at the end of the chamber to study the particles streaming out of the mirror during the plasma gun pulse and during the plasma decay.

Confinement Studies

1. Introduction .

In this chapter, we present data from the Constance II experiment which represent the operating regimes as we currently understand them. The introduction gives a brief description of the machine operation and presents the timing sequence of a typical shot. In the following sections we present data which characterize two regimes of operations; "long injection" discharges and "short injection" discharges. The plasma in these experiments, was generated in a 1/2" Ti-washer gun. Subsequent experiments with a pulsed gas gun showed qualitatively similar results. We discuss the conditions that are required to produce a mirror confined plasma of moderately high ion temperature and present characteristics of the resulting ion cyclotron instability. Finally, in this chapter we present the many other measurements that have been taken which characterize our plasmas geometry and evolution during a typical discharge. The data relating to ICRF and ECR heating experiments will not be presented in this chapter but are presented in their respective chapters.

The Constance II experiment is operated in a pulsed fashion, the shots are about 1 msec long and separated by approximately 2 minutes. Plasma is produced by a hydrogen loaded titanium washer gun or gas puffed gun of similar design. Plasma flows along the 2.5 meter long guide field into the mirror region where a fraction of this streaming plasma is trapped by collisions and wave turbulence. Plasma injection occurs for 0.1-1. millisecond. $50\mu sec$ before the termination of the plasma injection, a diverter coil located outside the mirror peak is energized. The purpose of the coil is to prevent plasma that has collected in the guide field during injection from streaming through the mirror region during the plasma decay period. Plasma which is not trapped in the mirror during injection flows into the end vacuum tank and strikes titanium gettered surfaces. Figure 3.1 shows a typical time sequence for the experiment. Titanium gettering is used throughout the experiment to help control the evolution of neutral gas during a shot. In general, neutral pressure is held below 5×10^{-6} for the duration of discharge, and virtually all of this gas production has been linked to plasma flowing into chamber walls, Ioffe bar coil supports, probes, etc. in the mirror chamber. With the quadrupole Ioffe bar coils turned off, the neutral pressure rises to a much smaller level.

The three groups of magnet coils are independently controllable over the following range; guide-field $\lesssim 1.8kG$, midplane-field $\lesssim 5.5kG$ midplane, quadrupole field ellipticity $\lesssim$ 20:1. The data presented in this chapter were taken with the guide field set at 1.8 kG, and a mirror midplane field of 2.8 kG with an ellipcity of 12.

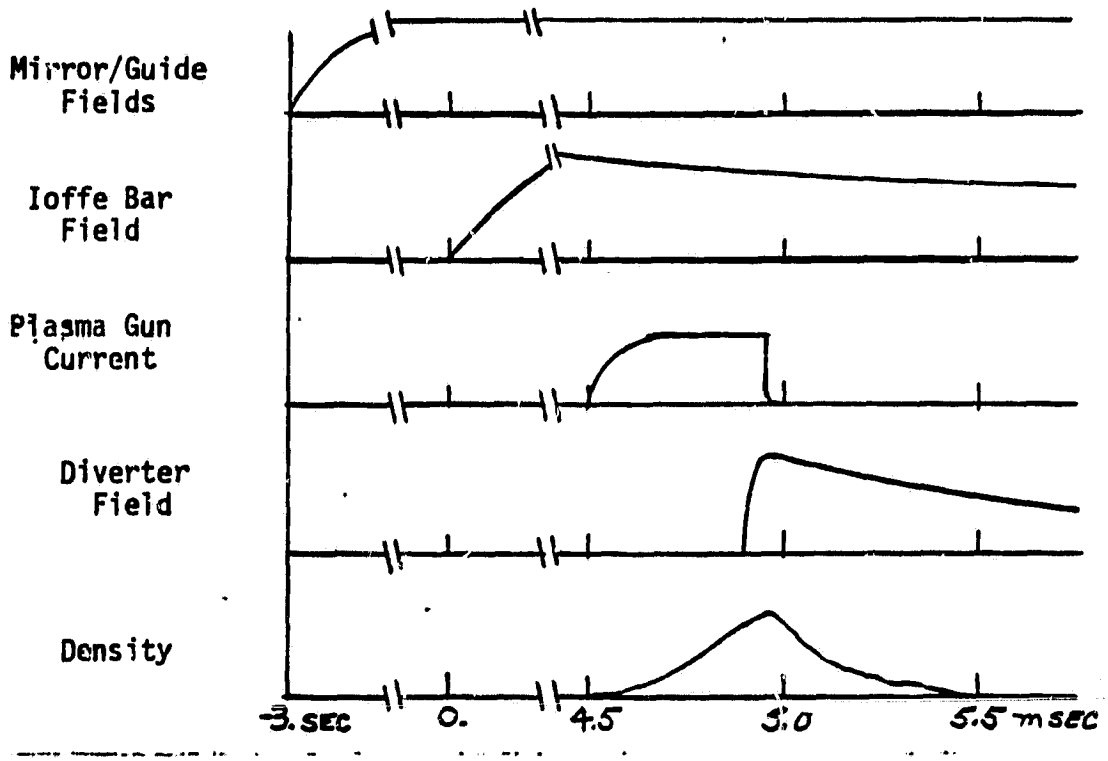

Figure 3.1. Typical timing sequence for Constance II shot.

2. Typical Discharges .

In this section we present and discuss the data from two sets of shots that are representative of the discharges obtained on the Constance II experiment using a 1/2" titanium washer gun. The first set of data is the average of nine consecutive shots taken under identical conditions and is characteristic of "long injection" shots. The plasma injection time was 375 μsec and the plasma gun capacitor bank was charged to 2000 volts. The data are presented in Figures 3.2 through 3.4. The second set of data is the average of six shots with a shorter injection time of 250 μsec and voltage of 2000 volts on the gun capacitor bank. These shots are characteristic of "short injection" shots. These data will be presented later in this section.

In the first data set, (*ie.* "long injection") Figure 3.2, the line density rises to a peak value of $1.9 \times 10^{13} cm^{-2}$ at the time of gun crowbar. The density then decays with a time constant of approximately 50 μsec. Charge exchange flux signals from two energy channels of the charge exchange analyzer are also shown. These two signals were used to calculate the ion temperature shown in Figure 3.2 characteristic of the CX flux above 500eV. The charge exchange signals are related to several plasma parameters through the relationship

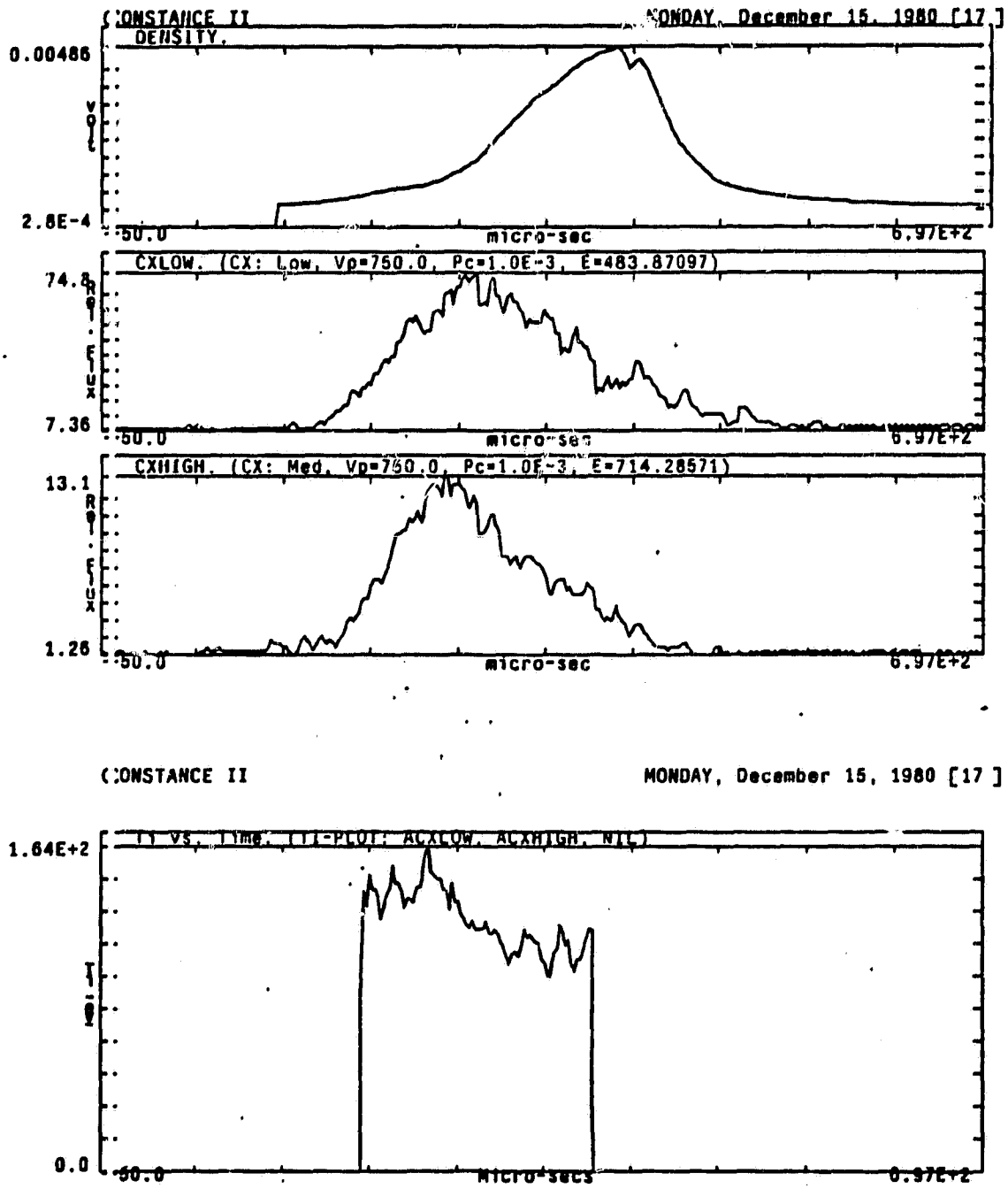

Figure 3.2. Average of nine shots characteristic of "long injection" shots.

$$CX_{Flux} = Cn_o n_i \frac{1}{E} exp(-E/kT)$$

where n_o is the neutral background density, n_i is the ion density, E is the energy of the channel, T is the ion temperature and C is a constant which includes the charge exchange and stripping cross sections, and the calibration of the instrument. It is clear from the above relationship that the ion density, n_i, at a given energy can be measured if n_o, and T are known. T is determined from the ratio of the signals from the two channels

$$kT = \frac{ln(CX_{low}/CX_{high})}{E_{high} - E_{low}}.$$

We have been able to measure n_o as a function of time by intentionally backfilling the vacuum chamber with a known density of H_2 gas and observing the increased change exchange flux in each of the energy channels. The neutral density n_o prior to backfilling is then related to backfilled case by

$$n_o = \frac{CX_n(t)}{CX_N(t) - CX_n(t)} N_o,$$

where N_o is the known backfill density, and CX_n, CX_N are the charge exchange flux signals corresponding to the neutral densities n_o and N_o respectively. Backfilling the vacuum chamber to a low density $N_o \approx 10^{11} cm^{-3}$ has also been valuable in enhancing the observed charge exchange flux early in the discharge when n_o is very low. We note here that the charge exchange flux measured by our analyzer is only an indication of ion density above 500eV. Our plasma is probably composed of a hot ion component and cold ion component as explained later. Therefore, we will refer to the ion density measured by the CX analyzer as the "hot ion density".

We present two additional pieces of data. Figure 3.4 shows the neutral density measured as a function of time using the technique described above. In Figure 3.3 we show the data from an average of nine shots taken under the same conditions as the data in Figure 3.2 except that the vacuum chamber was intentionally backfilled to a pressure of $3.2 \times 10^{-6} torr H_2$. In addition we show the total pressure (backfill plus plasma produced) and the corrected CX signal which indicates the true time history of the trapped hot-ion density $n^{hot}_{trap}(E)$ where E is the energy of the respective channels. We note here that the charge exchange diagnostic measures only the charge exchange neutrals that originated as deeply trapped ions since it views the plasma at the mirror midplane and at 90° to the magnetic field. That is, it only views neutrals that satisfy $v_{\|} \approx 0$, $v_{\perp} = \sqrt{2E/m_i}$ where E is the energy of the channel.

The trapped hot-ion density, n^{hot}_{trap}, is given by the following rate equation

$$\frac{d}{dt} n^{hot}_{trap} = \frac{n^{hot}_{stream}}{\tau_{trap}} - \frac{n^{hot}_{trap}}{\tau_{loss}} \qquad (3.1)$$

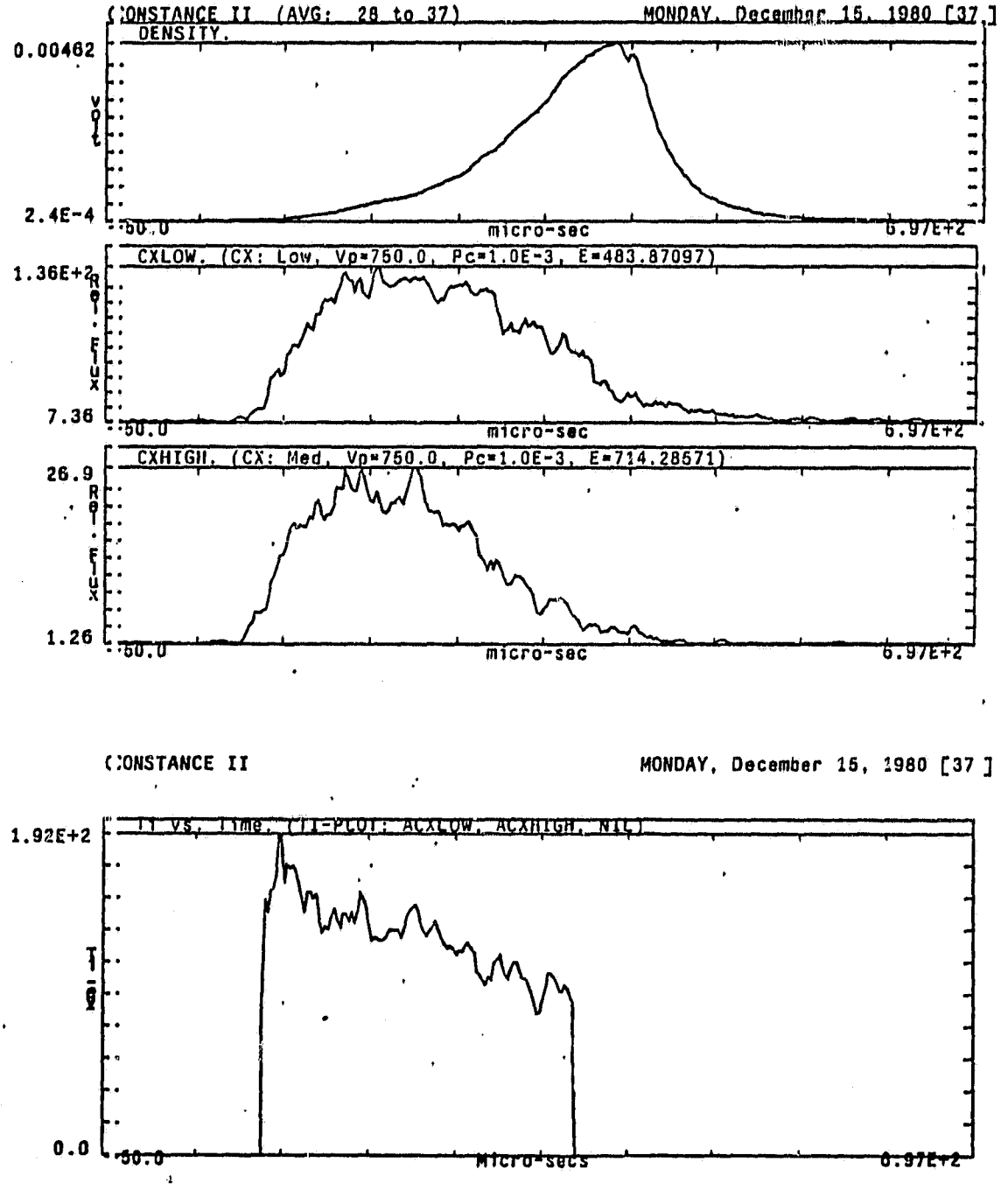

Figure 3.3. Average of nine long injection shots with the vacuum chamber backfilled to 3.2×10^{-6}torr.

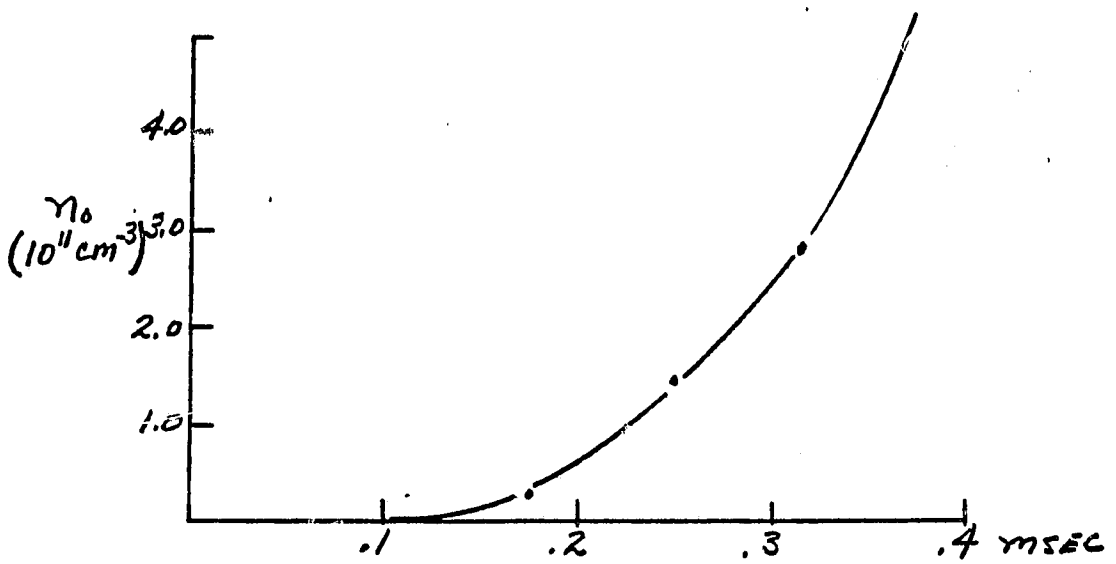

Figure 3.4. Neutral density as a function of time using the technique of relative CX intensity measurements as the chamber is backfilled with hydrogen.

where n^{hot}_{stream} is the density of streaming hot plasma (produced by the plasma gun). Referring again to Figure 3.3 it is clear that n_{trap} reaches a maximum at about 150μsec into the discharge, for the two energies being measured. At this time, the two terms on the left hand side of equation 3.1 must be equal, making $dn_{trap}/dt = 0$. The trapping and loss rates τ_{trap}, τ_{loss} are both diffusive processes in velocity space, resulting from collisions and RF or turbulent diffusion. While we do not know what τ_{trap} and τ_{loss} are quantitatively, during the filling process, they may be nearly equal since the diffusive processes which trap streaming-ions also result in loss of trapped-ions. The above argument leads us to the following conclusions about the present operation of Ti-washer gun operation and the filling process of the Constance II experiment. Early in the gun discharge the current of hot ions reaching the mirror rises rapidly to a peak value. The hot ion current then decreases with time, however, the trapped hot density continues to rise and at a $t = t_{max}$ the hot ion streaming density, n^{hot}_{stream}, equals the trapped density n^{hot}_{trap}. From this time forward, both n^{hot}_{trap} and n^{hot}_{stream} decrease monotonically with time. The density continues rise but this is due to colder, streaming ions. This scenario is summarized in Figure 3.5.

To establish a useful mirror confined plasma, we must maximize the density of trapped energetic ions and minimize the various collisional loss processes. The data presented thus far indicate that this optimum operation is obtained by injecting for a time t_{max} as indicated in Figure 3.5. We present data from

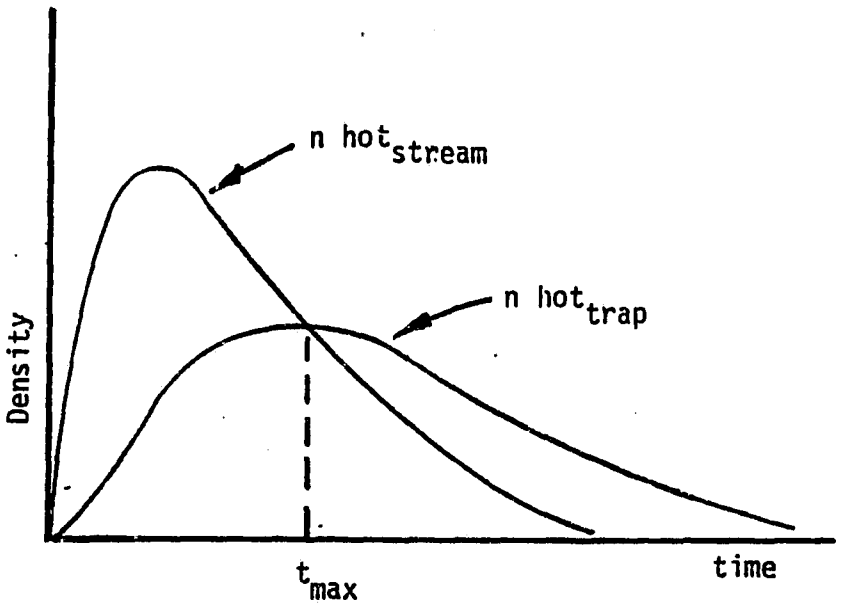

Figure 3.5. The evolution of n^{hot}_{stream} and n^{hot}_{trap}.

a discharge of this type in what follows. However, some discussion is appropriate at this juncture on our ability to control n_{trap} and the time t_{max} for which n^{hot}_{trap} is maximized. Our primary control of plasma gun operation is through the voltage applied to the capacitor bank power supply for the gun. In general, we can state that over a range of voltages from 750v to 1500v, higher voltages result in shorter times for t_{max} and that relatively little change is observed in the maximum value of n^{hot}_{trap}. Outside this voltage range, the maximum attainable n^{hot}_{trap} is generally lower in value. However, other factors affect the operation of the gun and the values of t_{max} and n^{hot}_{trap}. The total number of discharges logged on a gun effects the condition of the Hydrogen loaded washer and hence effects t_{max} and n^{hot}_{trap}, albeit in a somewhat unpredictable way. Finally, the vacuum conditions of the machine and the surface conditions of the gun have proven to have effects, as yet not well understood. These issues will be presented in greater detail in the plasma gun studies section of this report.

We now present and discuss data from a series of "short injection" shots. These data are averages of several consecutive shots taken under identical conditions. The plasma gun injection parameters have been chosen to maximize the measured value of n^{hot}_{trap}. These data are presented in Figure 3.6. The charge exchange flux rises to a peak at approximately the time of gun crowbar. The peak fluxes measured in the two channels are approximately equal to the first set of data representative of the long injection shots. The measured line density is very low during most of the shot, being at or near our lowest detectable value of approximately $8 \times 10^{11} cm^{-2}$. Note that the line density rises to a peak value of $1.6 \times 10^{12} cm^{-2}$ at the

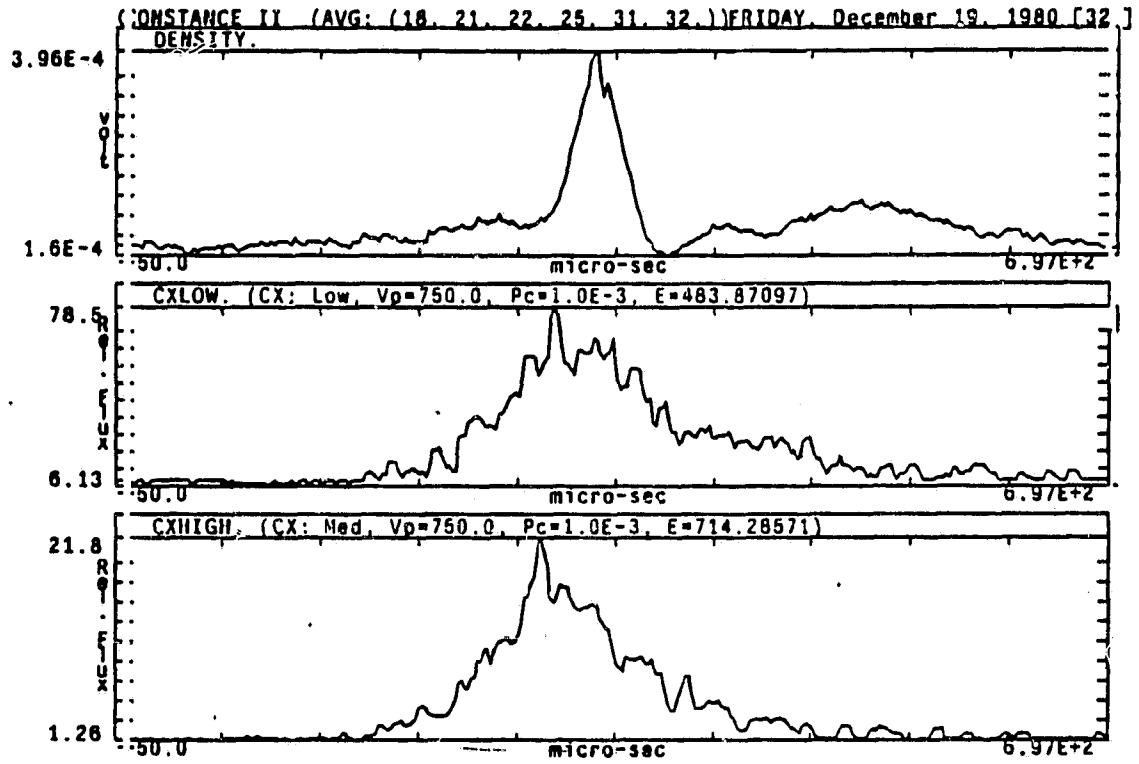

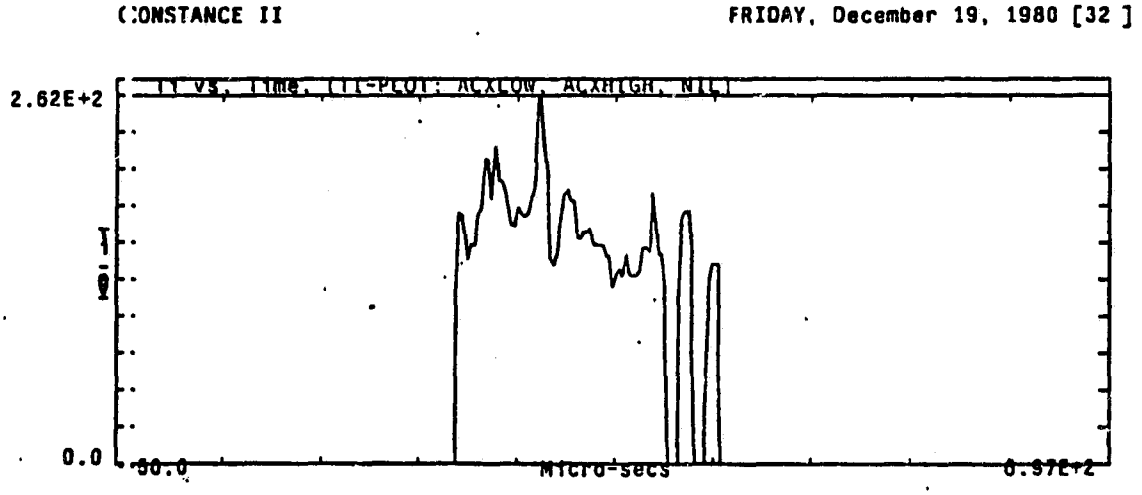

Figure 3.6. Average of seven shots illustrating "short injection".

time of crowbar, however this short duration of increased density is not consistent with the time history of the CX flux and therefore cold or unconfined plasma is probably responsible for this rise in density.

If we take the charge exchange decay time to be equal to the trapped density decay time (this is not strictly correct since we should correct for variation of $n_o(t)$), we can calculate the expected trapped density assuming classical losses due to ion-ion, electron drag, and charge exchange collisions.

$$\frac{1}{\tau_{conf}} = \frac{1}{\tau_{ii} \log R_{eff}} + \frac{1}{\tau_{drag}} + \frac{1}{\tau_{ex}}$$

R_{eff} is the effective mirror ratio $R/(1 + \phi/\tau_i)$ which accounts for a positive potential of ϕ at the midplane. We have taken a potential $\phi \simeq 4T_e = 20$ volts, $E_i = 150eV$, and the measured confinement time $\tau_{conf} = 200\mu sec$. Using their collision times given by [Ref. 1], we calculate an expected trapped density of $n_{trap} = 5 \times 10^{11} cm^{-2}$.

The conclusions can be summarized as follows. We have successfully produced a mirror confined plasmas of moderately high ion temperatures $T_i \simeq 150eV$ and line density of $nL \lesssim 8 \times 10^{11} cm^{-2}$. These plasmas exhibit confinement times which are consistent with collisional losses from a mirror R = 2. Attempts to increase the trapped density above $nL > 8 \times 10^{11} cm^{-2}$ result in the addition of a cold ion component and the reduction of the hot ion component. Densities of up to $nL \lesssim 6 \times 10^{13} cm^{-3}$ have been demonstrated with depressed ion temperatures and may be useful for ECRH studies. The above results have lead us to explore the operation of modified washer gun designs, and hot cathode guns which have proven more successful in similar experiments on PR-7 by Ioffe and co-workers (Ioffe, *et al.*, 1974).

3. The Characteristics of the Ion Cyclotron Fluctuations .

Our goal in studying the mirror trapped plasma in Constance II is to produce a plasma which reliably exhibits an instability of the kind routinely observed on higher energy density devices such as 2XIIB and TMX. We have described in the previous section the controls and parameter range available to us in the operation of Constance II using the 1/2 inch titanium washer gun as our plasma source. From the previous discussion we would expect that instabilities driven by an ion loss-cone distribution would be present only when operating in the "short injection" and therefore low density mode. We have found this to be a necessary however not sufficient requirement for observing ion cyclotron fluctuations during the plasma decay. The utmost care and vacuum integrity is also an important ingredient for exciting loss-cone driven instabilities in experiments of moderate ion temperatures (100-1000eV). We have observed this to be the case on previous experiments, Klinkowstein, [Ref. 22], Mauel, [Ref. 25], and it has been reported by others [Ref. 18].

Shown in Figure 3.7 is an oscilloscope photo of the signal from a floating potential probe, located at the mirror midplane, during the plasma decay of a short injection discharge. The probe contacts the plasma

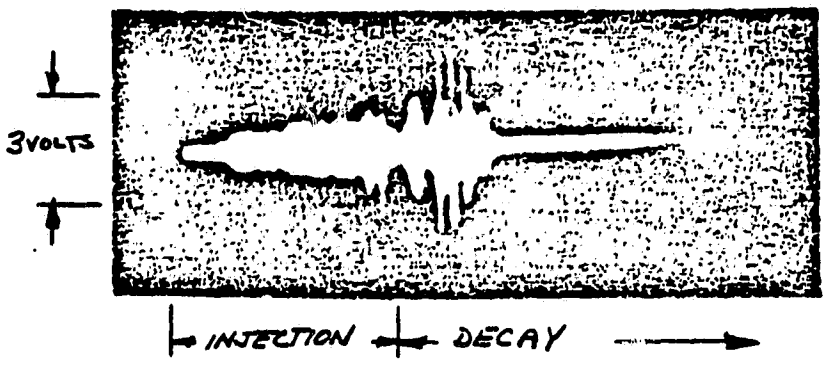

Figure 3.7. Oscilloscope photo of the signal from a floating potential probe, located at the mirror midplane, during the plasma decay of a short injection discharge.

at its edge ($r = 3cm$). During the injection phase of the experiment, fluctuations are detected which are broad in spectrum and associated with the discharge mechanism of the plasma gun. Immediately following gun crowbar and the energizing of the diverter coil, a quiescent stage of the plasma decay is observed usually lasting $50 - 150\mu sec$. A burst of fluctuations is then observed. The fluctuations during the plasma decay are at the ion cyclotron frequency and its harmonics. Shown in Figure 3.8 is a burst of ion cyclotron fluctuations that was captured by one of our high frequency digitizers and the associated Fourier transform of this signal. Note that peaks are observed close to the calculated midplane ion cyclotron frequency.

As mentioned earlier, the fluctuations are observed only under the best of vacuum condition and for short injection duration. We do not observe these fluctuations for longer injection discharges. This is consistent with the increased collisionality associated with the high density cold ion component that we measure under these conditions.

4. Other Plasma Parameters .

In addition to the plasma parameters already discussed several other measurements have been made to characterize the Constance II plasma. A Langmuir probe located at the mirror midplane was used to

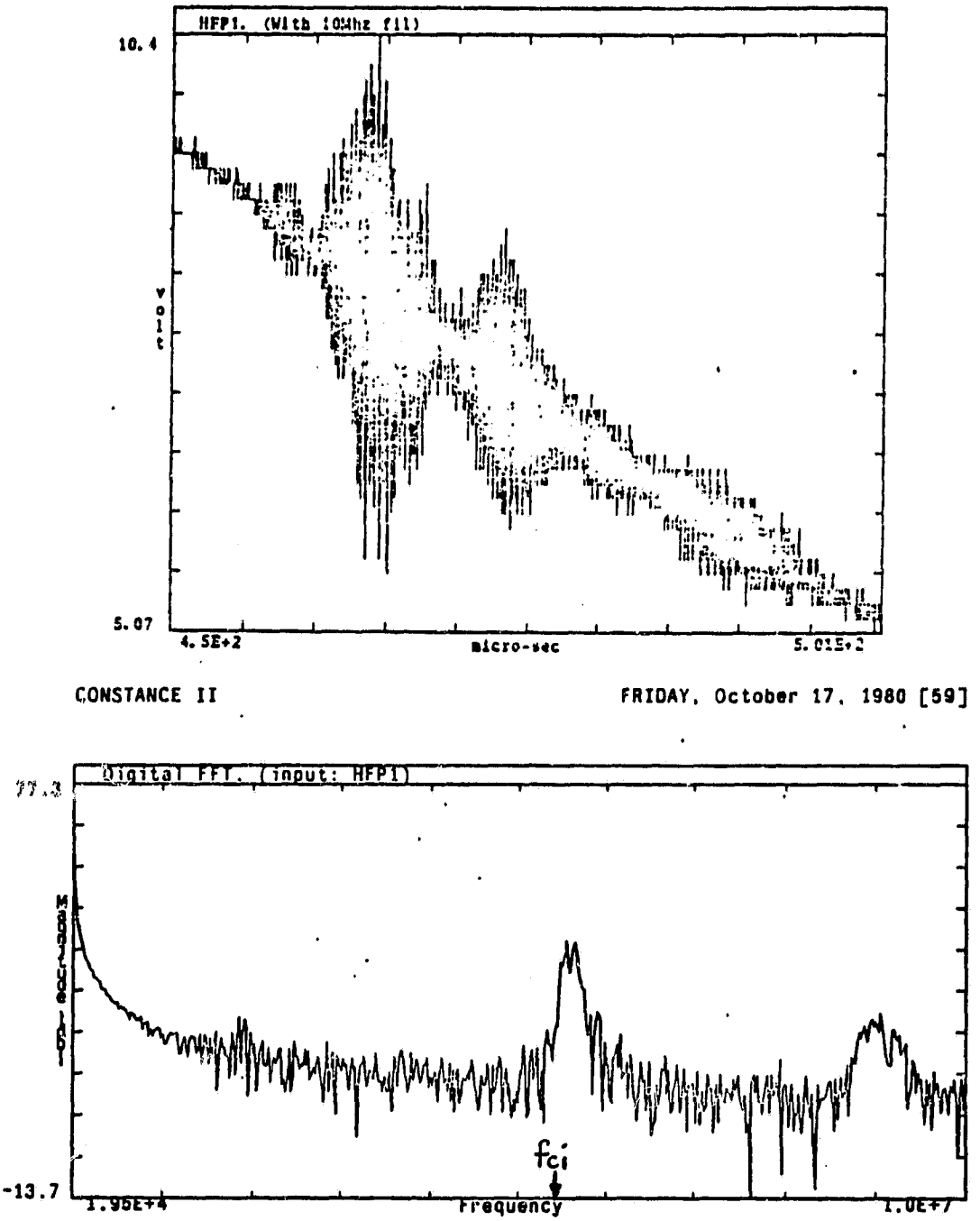

Figure 3.8. A burst of ion cyclotron fluctuations captured by a high frequency digitizer (top) and the Fourier transform of this signal (bottom). The second peak is due to the aliasing of the second ion-cyclotron harmonic.

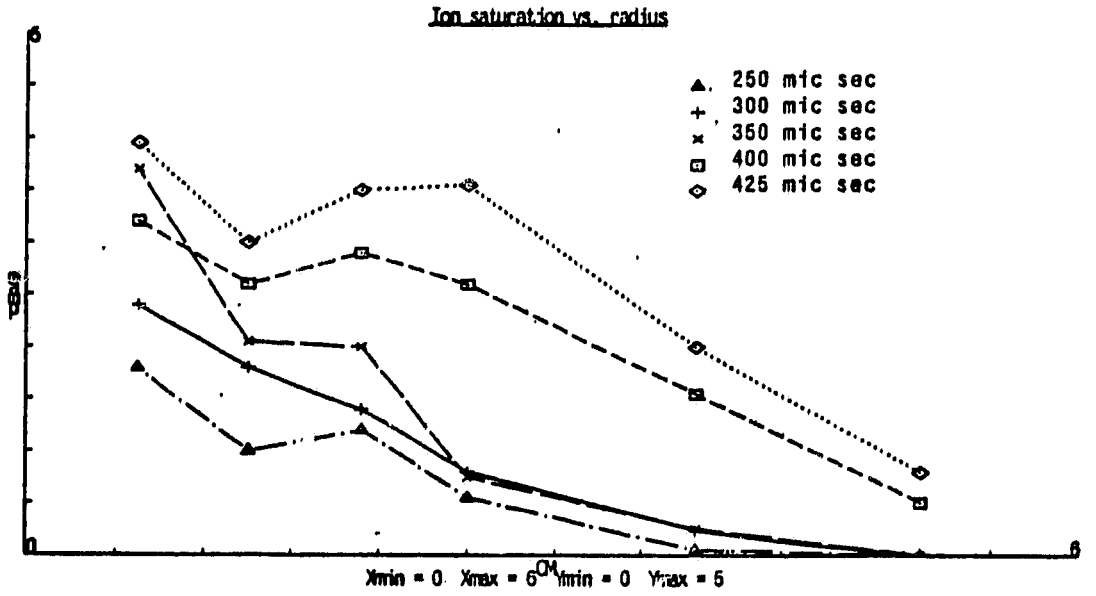

Figure 3.9. Ion saturation current as a function of radius and time with Ioffe bars energized.

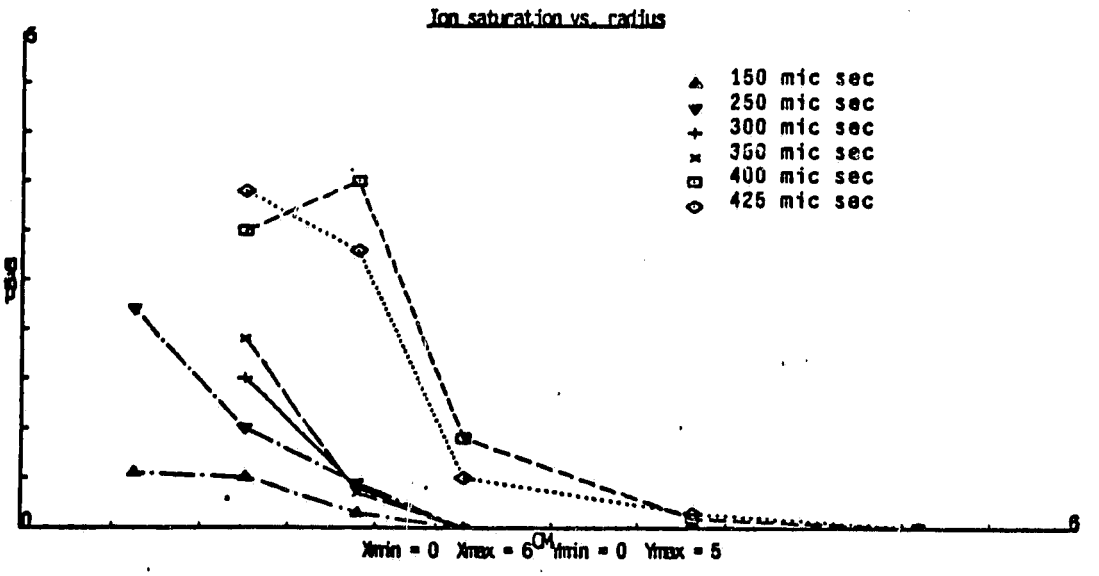

Figure 3.10. Ion saturation current as a function of radius and time without Ioffe bars.

measure the radial density profile, and to determine T_e as a function of time. Shown in Figure 3.9 and 3.10 are the ion saturation current as a function of radius and time, for two plasma injection conditions. Figure 3.9 is with the Ioffe bar coil energized and Figure 3.10 is without the Ioffe bar field. The most immediate difference between the two cases is the larger radial extent of the plasma when the Ioffe bar coils are on. The Ioffe bar field also has a marked effect on the measured trapped, hot-ion density. In the absence of the Ioffe field, the trapped, hot-ion density is below the sensitivity of our charge exchange analyzer even when the chamber is backfilled with H_2 to levels higher than those with the Ioffe bars energized. This indicates that trapped, hot-ion density is increased by more than 100 times when the quadrapole field is on.

The Langmuir probe bias voltage can be swept through to 600 volts in $7\mu sec$. It has been used to measure the electron temperature during the Constance II discharge. The electron temperature is generally in the range of 15-40eV during the injection phase of the experiment and somewhat colder 4-15eV during the plasma decay. Figure 3.11 shows the electron temperature for gettered and ungettered vacuum chamber conditions. A slight increase in Te was observed for the gettered case. Also shown, Figure 3.11, is a parametric plot of probe current vs. bias voltage for a typical probe sweep.

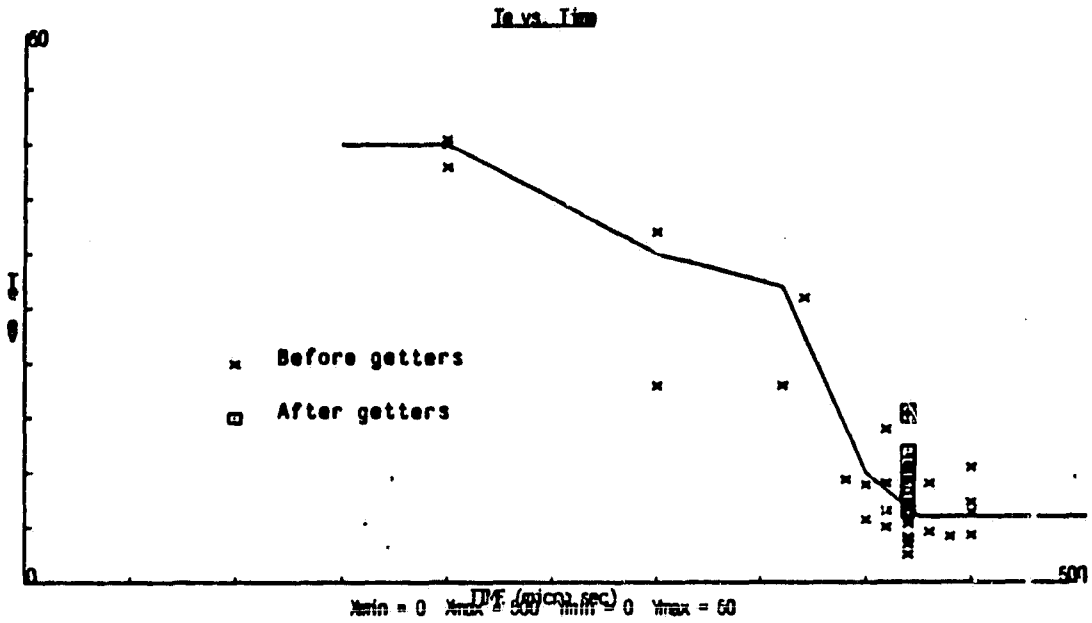

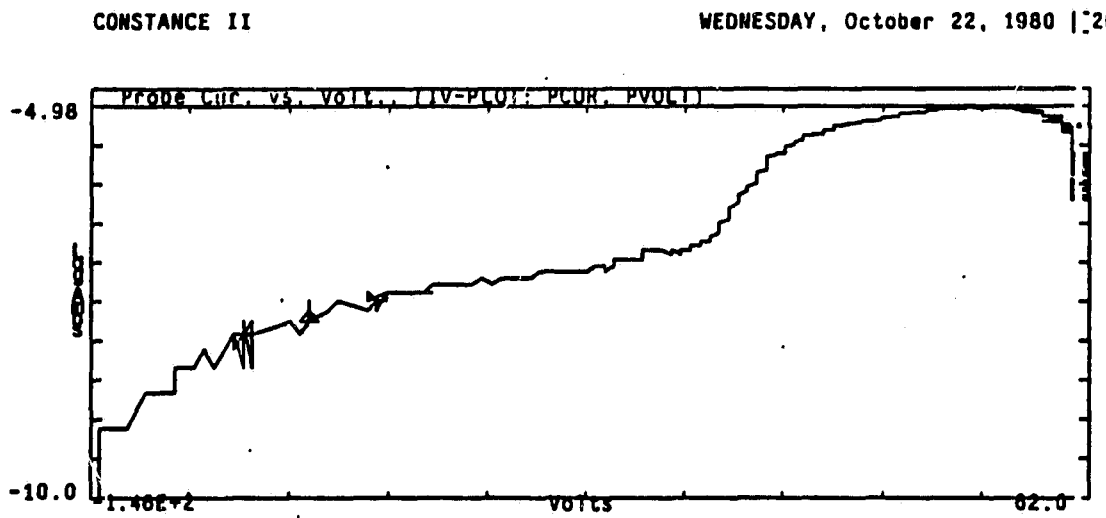

Figure 3.11. The electron temperature for gettered and ungettered vacuum chamber conditions. Also shown is a parametric plot of probe current vs. bias voltage for a typical probe sweep.

ICRF Program

1. Introduction .

An ICRF heating program has been undertaken on the Constance II experiment with a primary objective of better controlling the mirror trapped plasma parameters. In the absence of ICRF heating, plasma parameter adjustments are possible only by changing the plasma gun power supply settings. The ion population can be altered in several ways using ICRF heating. Bulk heating of ions is possible by resonant absorption of the slow ion cyclotron wave. Trapped plasma density can be increased due to enhanced diffusion of ions in velocity space. Finally, the ion distribution can be broadened or peaked in velocity space by changing the location of the resonance zone in the mirror.

Our initial ICRF heating results have shown that we can successfully heat the ion population up to 450eV by the application of 50kW of RF power resonant near the midplane of the mirror. In addition, the data from the microwave interferometer imply that the trapped density is increased substantially by the application of the ICRF heating.

2. ICRF Transmitter .

A 5 MHz 150kW transmitter was constructed to perform the ion cyclotron heating experiments. This transmitter was constructed from surplus parts collected from the Plasma Fusion Center and the Research Laboratory of Electronics at M.I.T. The circuit design is a two stage class C amplifier. A schematic of the circuit is shown in Figure 4.1. The first stage consists of six 6l46B pentodes operating in parallel and produces a maximum output of approximately 1kW. These tubes drive the output stage which consists of a single EIMAC 4CX15000 air cooled tetrode. This tube is capable of delivering 150kW in a short pulse mode. The plate power supplies of both amplifier stages are capacitors which are charged by power supplies of modest rating. The transmitter can supply its full output for 1 msec.

The antenna used to couple power to the plasma is a two turn loop antenna insulated with Kapton and woven glass. The design is illustrated in Figure 4.2. The unloaded Q of the antenna is 150. The antenna is located 15 cm from the mirror midplane and the long dimension of the loop is in the direction of the plasma fan. The dimensions of the antenna were determined by Langmuir probe measurements of the plasma at the location of the antenna. Figure 4.3 shows the ion saturation current as a function of radius. The dimension of the antenna loop was chosen to be $r = \pm 3.5cm$ so that plasma would not intersect the antenna, but coupling to the plasma would be maximized.

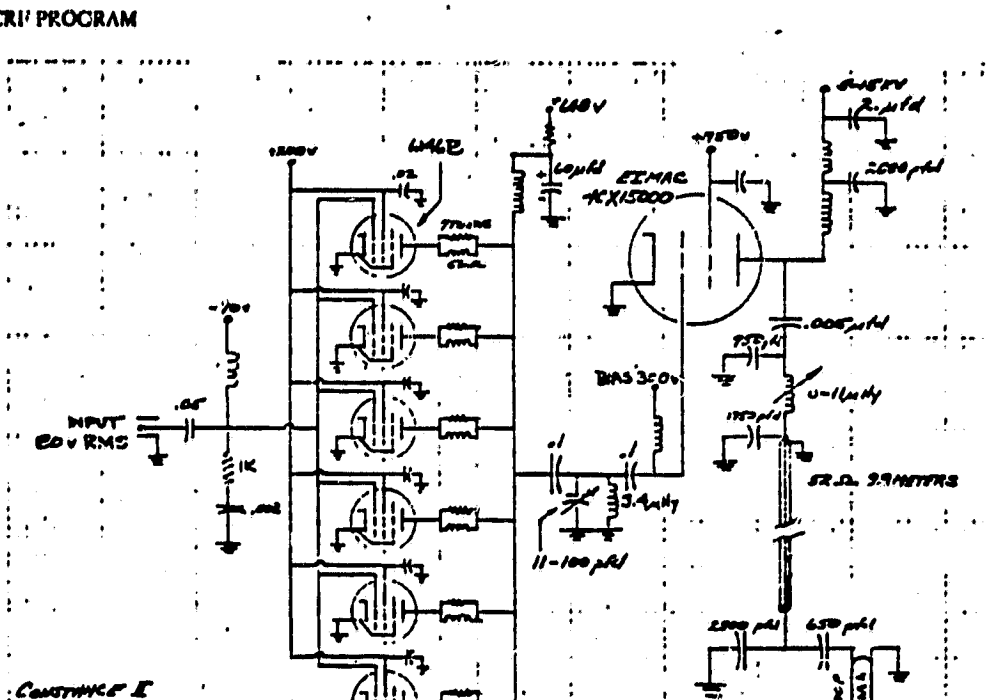

Figure 4.1. Schematic of the 100kWatt ICRF generator.

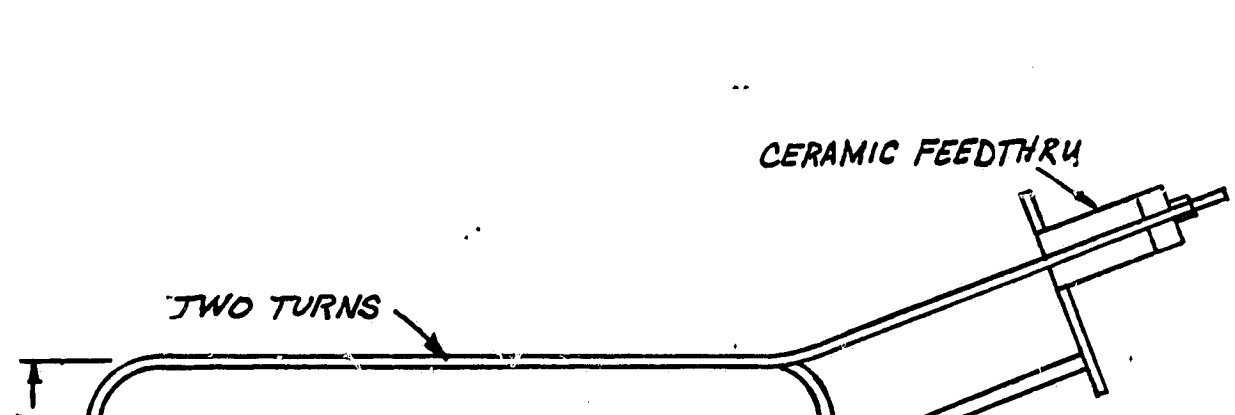

Figure 4.2. Illustration of ICRF antenna design.

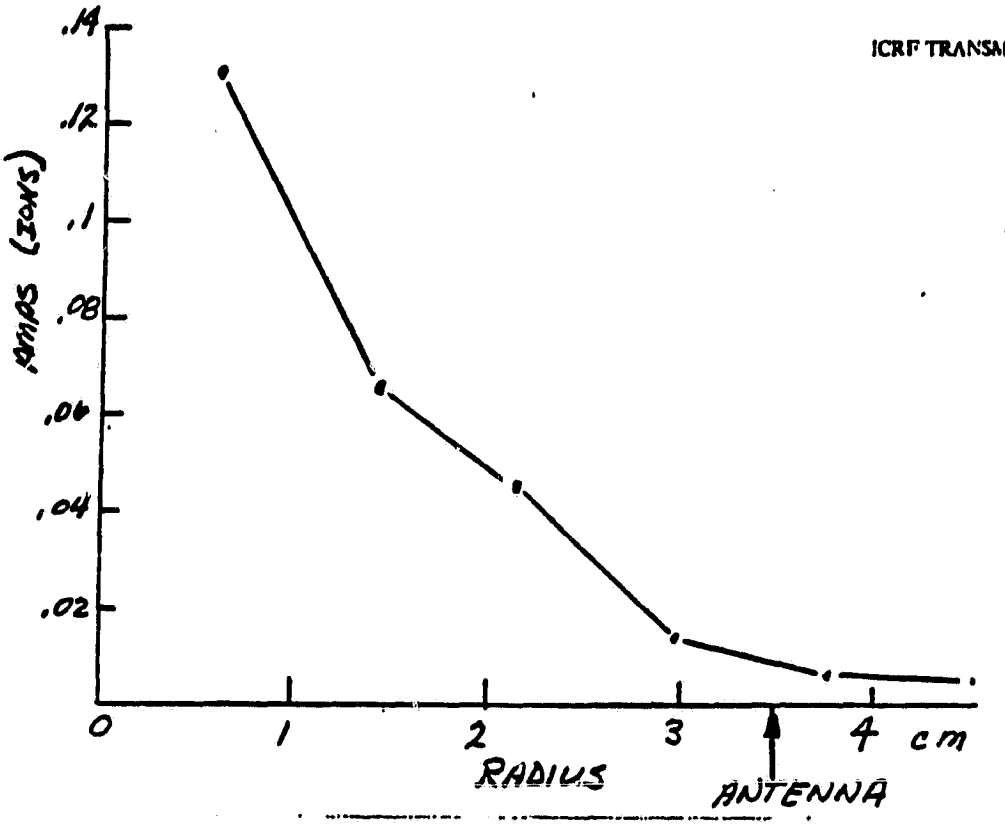

Figure 4.3. Ion saturation current vs. radius near antenna.

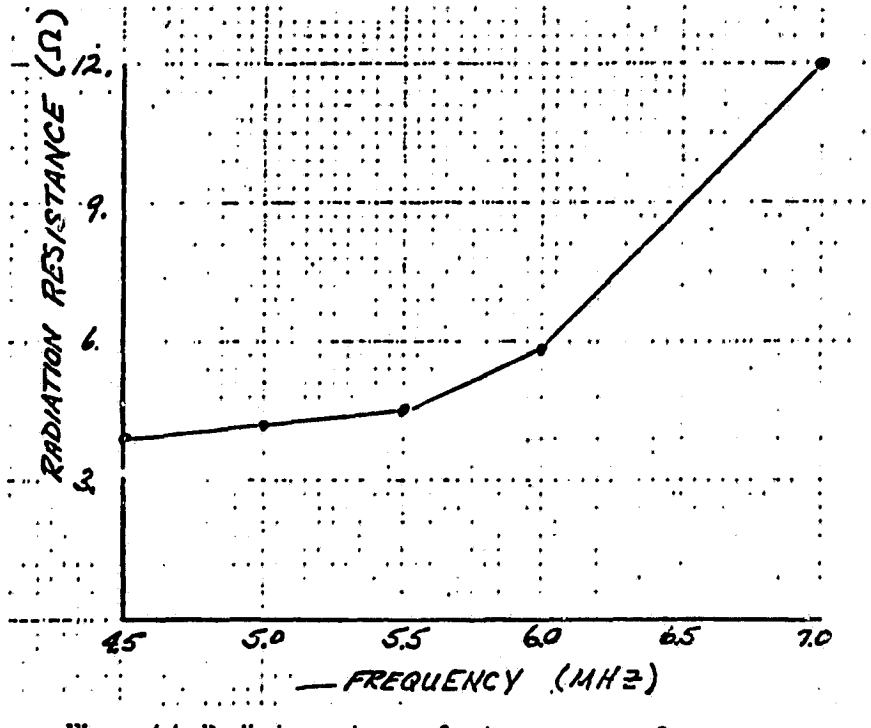

Figure 4.4. Radiation resistance for the antenna vs. frequency.

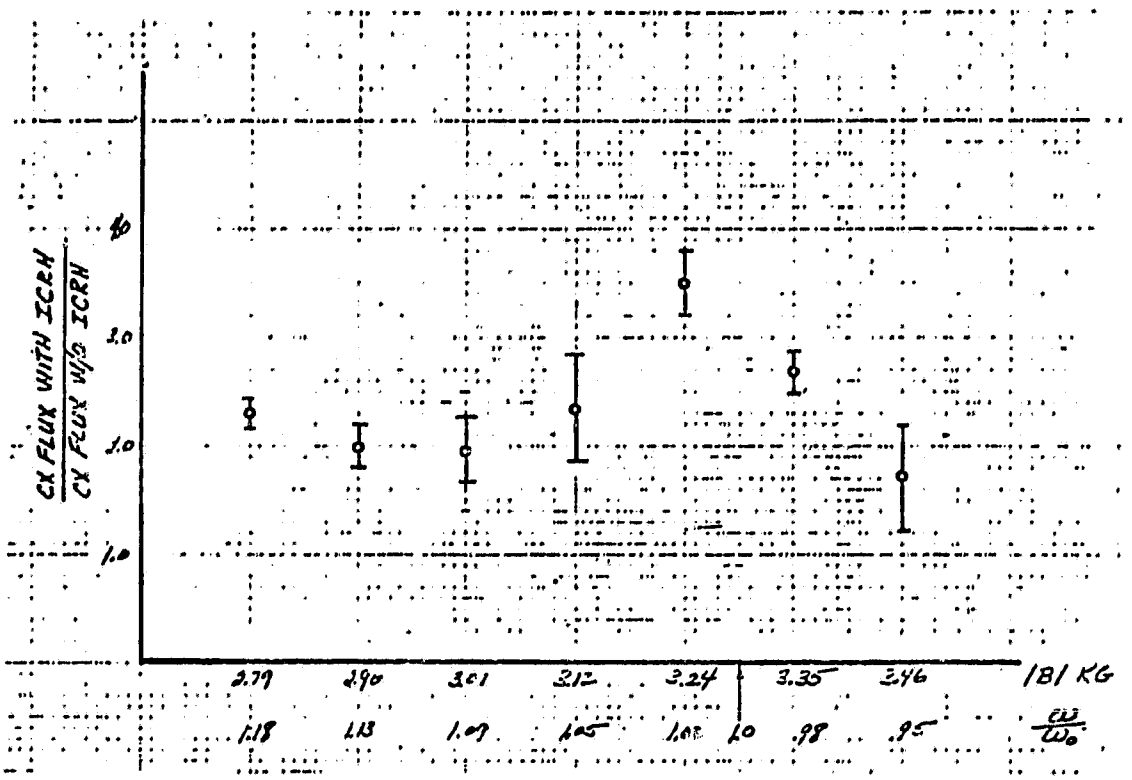

Figure 4.5. Increased CX flux due to ICRF.

In order to properly match the antenna to the transmitter, low power plasma loading experiments were performed with a single turn loop antenna and later repeated with the two turn antenna. The radiation impedance was measured as a function of frequency. The data for the two turn antenna are shown in Figure 4.4. A Pi matching network was used to match the 500 ohm output impedance of the 4CX15000 tube to a 52 ohm transmission line. The antenna impedance of 5 + j66 ohms was then matched to the transmission line using a capacitive network as shown in Figure 4.1. The transmission line is 9.9 meters long and is essentially lossless when compared to the antenna loss in the presence of the plasma.

3. Heating Results .

ICRF heating of the Constance II plasma has been performed for RF power levels of up to 50 kW. The ICRF heating pulse is coincident with the plasma gun injection time. The heating pulse is 200-500 μsec long. The maximum power level of 50 kW is limited by breakdown of the ceramic feedthrough insulation of the antenna. Maximum heating, as observed by the charge exchange analyzer, was obtained when the heating frequency was tuned near the mirror midplane field ($\omega/\omega_{ci} = 1.02$). However, heating has been observed for frequencies $.95 < \omega/\omega_{co} < 1.2$. Figure 4.5 shows the increased charge exchange signal observed in the 500eV charge exchange channel as the frequency is tuned through the midplane resonance.

We have measured the charge exchange flux as a function of energy to determine the increase in

average ion energy resulting from the application of ICRF heating. For a 50kW heating power level, the ion temperature increases from 265eV to 460eV. The charge exchange spectrum data are shown in Figure 4.6.

The initial heating results have not shown a noticeable increase in ion cyclotron fluctuation levels associated with the DCI.C instability. However, more data must be taken before we can be sure about the effect of heating on the instability. We are investigating the effect of ICRF heating on the ion distribution function. The growth rate of the instability is dependent on the detailed nature of the distribution function, and the application of ion heating may alter the distribution in such a way to have a stabilizing effect. A Monte Carlo code is being written to include the effects of ICRF heating so that we can better understand the effect of heating on the ion distribution.

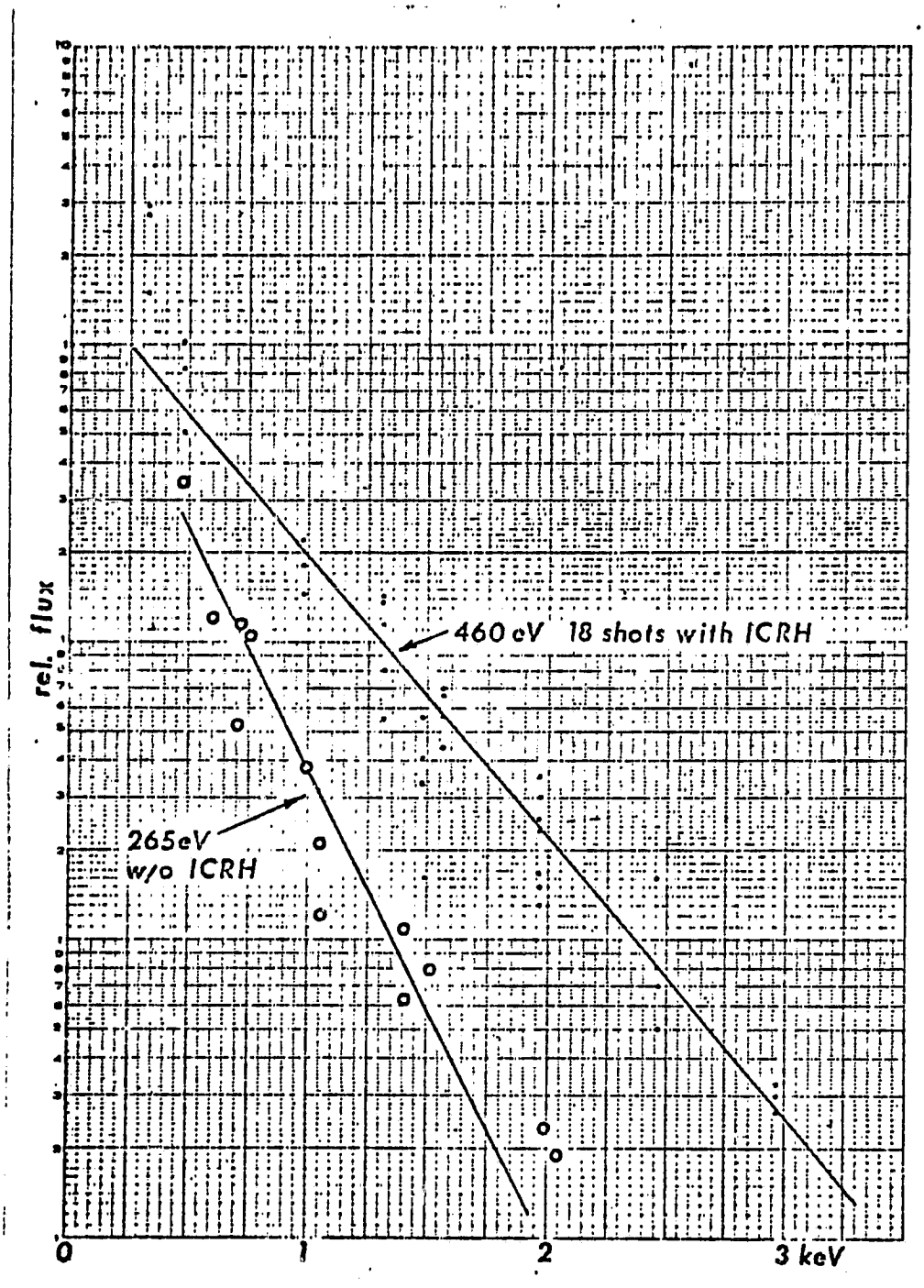

Figure 4.6. Charge exchange spectrum with and without ICRF.

ECRH Program

The prime goal of the Constance II electron cyclotron resonance heating (ECRH) program is to develop a basic understanding of the physics of heating dense ($\omega_{pe} \gtrsim \omega_{ce}$) and moderately warm ($T_e \gtrsim 20eV$) mirror-confined plasmas. Once this heating process has been successfully understood, it should be possible to explain and predict the evolution of the electron energy distributions in the presence of RF. The experiment is well equipped to create and evaluate a hot electron thermal barrier, to study hot electron stabilization of microinstabilities, and to identify the hot electron instability observed at high heating powers. These are the four principle tasks which can be addressed by the ECRH experiments.

The details and plans of the ECRH program are organized into four sections. First, the microwave hardware, and basic heating configurations are described. Then, the experimental geometries and procedures for the four tasks are briefly summarized. In the second section, the expected behavior of the experiment during ECRH is previewed, while, in the third section, the data from the first round of heating experiments are presented.

1. Constance II ECRH Facilities and Procedures .

Constance II has a high power, 9.3 GHz Varian Magnetron which has been adapted for use in a single, long-pulse mode. The magnetron along with the electron diagnostics described earlier provides a facility for the evaluation of ECRH in mirrors.

The microwave source is the same Model SFD-303, 3 cm, $1MW$ coaxial magnetron (on loan from Varian Associates) used to stabilize ion-cyclotron fluctuations in the Constance I ECRH experiments [Ref. 25]. A long-pulse, spark-gap modulator allows heating powers up to $200kW$ for $45\mu sec$. The forward and reflected powers are monitored by calibrated attenuators and detectors, and the waveguides are pressurized with SF_6 to avoid breakdown. In addition, the enlarged access of Constance II as compared to Constance I has allowed the launching horns to be located farther from the plasma boundary nearly eliminating the window breakdown observed in Constance I.

The first set of experiments (and those which are currently in progress) is designed to examine the physics of two launching geometries: (1) a side-launched, linearly polarized, extra-ordinary wave, and (2) an end-launched, right-hand circularly polarized, whistler wave. These two modes should have high first-pass absorption in the low to moderately hot electrons of Constance II and allow simple theoretical models to be used in analyzing the data. The waveguides and launching horns for these experiments are presently under

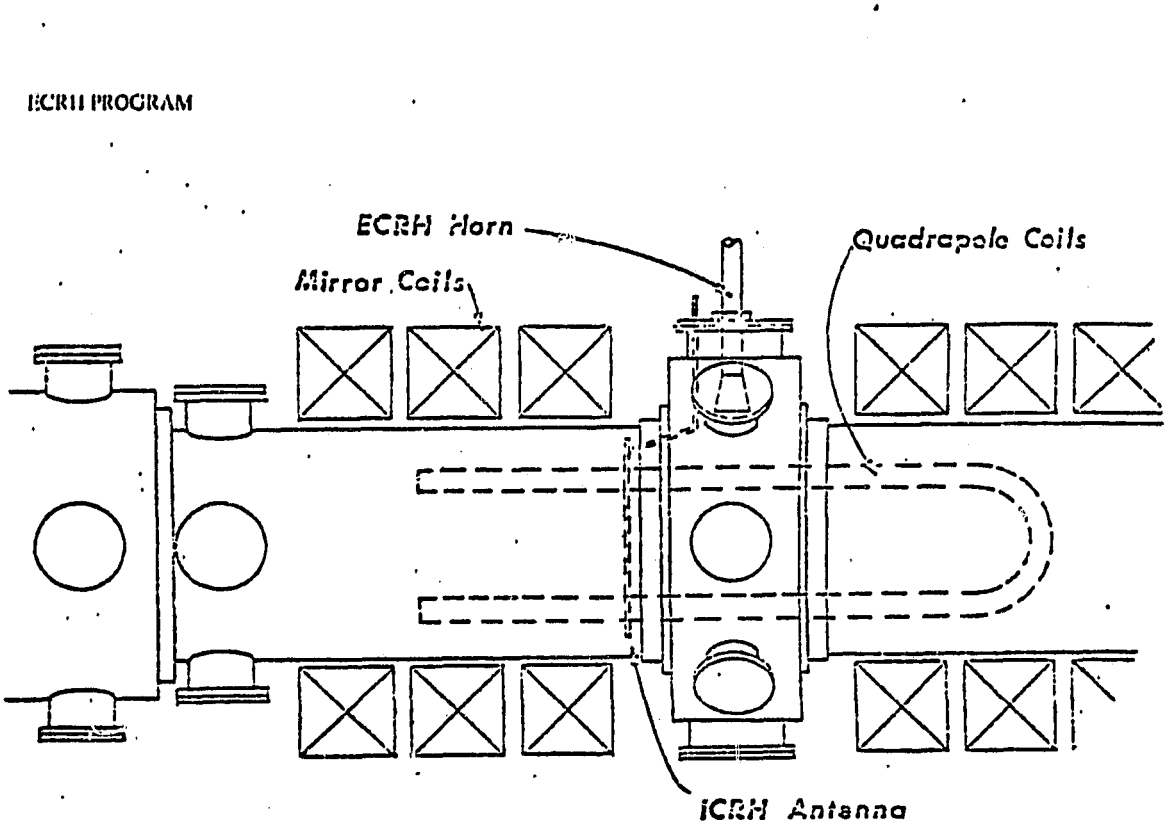

Figure 5.1. Waveguide geometry for the preliminary Constance II ECRH experiments discussed in Section 5.3.

construction. Temporarily, a horn has been placed in the mirror midplane as shown in Figure 5.1.

The objective of these first experiments is general and exploratory. They should determine experimentally the evolution of the electron energy distribution as plasma and heating parameters are varied. The x-ray, Thompson scattering, VUV, and magnetic and Langmuir probe diagnostics will determine the net power absorbed and the percentage of tail and bulk heating. All of the electron diagnostics except the VUV monochromator can be scanned either radially, axially, or both to estimate the density and location of "sloshing" electrons and the amount of edge heating. The microwave power and pulse length can be changed permitting the comparison of non-linear and quasi-linear heating and the determination of the energy confinement properties at any instant during the $45\mu sec$ heating pulse. Finally, the most versatile feature of the experiment is the wide range of plasma densities and magnetic fields over which a target for the ECRH can be produced. The variation of density allows direct comparison of overdense and underdense absorption. Raising or lowering the main magnetic field permit the heating of the plasma at either the first or second harmonic and the re-positioning of the resonant zones to any axial position within the mirror.

Another set of experiments can be performed in conjunction with the E-beams studies. The scaling of the heating properties with the initial electron temperature might be experimentally determined by "pre-heating" the electrons during plasma buildup with a controlled injection of the E-beam. By initially warming

the electrons, the most serious limit to the direct application of the Constance II ECRH results to future experiments, namely the low to moderate electron temperature, may possibly be extended.

After cataloguing the effects of ECRH, the machine will be in a position to address the three specific problems or applications of ECRH discussed in the introduction. These are (1) to create and evaluate a hot electron thermal barrier, (2) to study hot electron stabilization of microinstabilities, and (3) to identify the hot electron instability observed at high heating powers. The order and extent to which these projects will be undertaken depends both upon the outcome of the preliminary ECRH study and upon the outcome of the confinement studies (hopefully, producing a dense, DCLC unstable plasma). At this time, only a brief listing of the possibilities for the second half of the ECRH program is presented.

First, a hot-electron thermal-barrier can be created using a design similar to that proposed for TMX-upgrade. By reconnecting the mirror coils we can produce a 4:1 mirror ratio instead of its present value of 2:1. Then, the same microwave plumbing used for the heating experiments will be used simultaneously to heat the midplane barrier electron at the second harmonic and the outboard "bulk" electrons at the first harmonic. The variable power splitter will be used to enable both horns to be powered from the same (and only) magnetron while still permitting complete control over relative intensity at each region. If "sloshing-ions" can be produced by the ICRF, the energy required to maintain the barrier will be compared to that needed with and without ICRF. To test and evaluate the barrier, a large stainless steel paddle will be inserted near one of the mirror peaks purposely cooling the un-heated half of the mirror plasma. Langmuir probes positioned on either side of the barrier will be able to measure the difference of the local electron temperatures as a function of barrier density and temperature.

Secondly, hot electron stabilization of DCLC can be studied in the same manner as used previously by Klinkowstein [Ref. 22] and Mauel [Ref. 25] on Constance I. However, Constance II is armed with superior diagnostics and (hopefully, by the time these experiments are fully underway) a thorough understanding of the capabilities of ECRH. In addition, the simultaneous progress of the E-beam studies should allow direct comparison of E-beam and ECRH stabilization under identical conditions. The objectives of the stabilization experiments will then be straightforward. First, those specific heating conditions (e.g. power, pulse timing, and resonant zero location) which stabilize the fluctuations will be identified systematically. Then, using the same methods used during the exploratory ECRH experiments, the electron energy distribution, axial electron location, axial potential variation, and neutral gas pressure present during the moments of stabilization will be analyzed. It should be possible to combine these data with past results and with the recent theory of Gerver [Ref. 13] to generate a consistent experimental picture of the mechanism responsible for the hot electron stabilization observed in Constance II.

Finally, the last possibility currently planned for ECRH at Constance II is the identification of the hot electron instability which has been observed at high heating powers on both Constance I and Constance II. The conditions for the onset of the instability would be labeled by varying density, heating power, and heating zone location. The frequencies, wavenumbers (for the electrostatic modes), and bandwidths of the instability will be measured using techniques similar to those described in the section on gun studies. In addition, the detrimental effect of the instability on the electron confinement will be measured using

diamagnetic loops and x-ray diagnostics.

2. A Theoretical Preview of ECRH .

The theory which will be used to interpret and analyze the Constance II ECRH data falls into three categories. It must determine (1) the route followed by the waves, traveling from the launching horns to the point of absorption, (2) the mechanism by which the particles absorb the wave energy, and (3) the global energy balance between the waves, electrons, and the electron's collisional losses. This section briefly reviews these three theoretical problems for the purpose of clarifying the issues facing the experiment and assisting the description of the preliminary data in the following section.

Porkolab [Ref. 36] studied the ray trajectories, accessibility conditions, and refraction patterns of electron cyclotron waves propagating in mirror geometry. By using the simple linear model of cyclotron damping, they have been able to estimate the initial power absorption of the waves by a locally Maxwellian plasma. This work is immediately useful to the Constance II ECRH experiment. For example, from a CMA diagram, it is found that the right-hand circularly polarized (whistler) wave is always accessible provided the wave is launched from the high field region of the mirror. The extraordinary wave (with $k_{\|} = 0$) is accessible when launched from the high fields only to $\omega_{pe} < \omega_{ce}$. Then, using Porkolab's calculations for the power absorption [Ref. 11 and 35] the whistler wave is expected to be completely absorbed on the first passes; whereas, the extraordinary wave should be absorbed on the first pass only for electron temperature greater than about 300 to 700eV depending (in a complicated and critical way) upon the density, the magnetic field gradient, and the direction of propagation with respect to the magnetic field. Since Constance II has an initial electron temperature between 5 and 20eV, the side-launched waves will initially pass through or refract around the plasma. The rays will bounce within the chamber and get absorbed either by the high $k_{\|}$ modes, by making several pass through resonance, or by wall absorption. After the initial heating phase, the electrons are likely to be non-Maxwellian; nevertheless, as the temperature rises above 200eV, complete first pass absorption is expected.

The mechanism of linear cyclotron absorption used by Porkolab to estimate the RF damping is not useful, however, to model the time development of the electron energy distribution. This requires a detailed treatment of the bouncing orbits of the particles in the magnetic (and electrostatic) well and the stochastic diffusion resulting from the overlap of the wave particle bounce resonance [Ref. 23, 4, and 28]. Diffusion coefficients for the particles have resulted from these analyses and can be used with a Fokker-Planck code to predict the time response of the electrons to the ECRH. These theoretical studies are underway and should give details such as the heating rate, ECRH equilibrium, and turning-point accumulation. In addition, careful analysis of the power absorption mechanism gives a limit to the maximum power which permits valid application of the linear theory. For the experiments described in the next section the heating can be considered linear roughly when $P(kWatt) < 5T^{5/3}(kev)$. In other words, for $5kW$ heating, the average electron energy must be greater than 1 KeV. In most cases, the Constance II heating is highly non-linear. The heating rate, then, is given by the bounce rate of the particles and the average change in magnetic

moment on passing through resonance, [Ref. 28]. The non-linear heating scales approxiately as $P_{rf}^{1/2}$, and the linear heating rate scales as P_{rf}.

Finally, the remaining theoretical aspect of the ECRH heating to be considered is the confinement and loss properties of the heated electrons. These are predominantely the classical collisional mechanisms of the mirror in contact with the walls via an external plasma and the background of neutral gas [Ref. 1 and 27]. (Cyclotron and bremsstrahlung radiation should also be included here; however, for all temperatures expected in Constance II, these will be insignificant compared to collisional losses.) The possibility of an ECRH maintained equilibrium is of great importance to the barrier studies and will be investigated both experimentally and theoretically.

3. Preliminary Experimental Results

While construction of the diagnostics is being completed, preliminary data have been gathered in order to test the basic operation of the modulator. Heating has been successfully observed, and, in this section, preliminary "check-out" data are summarized [Ref. 26].

The geometry of the experiments was shown in Figure 5.1. The side-launched, extraordinary mode is used although the horn is placed in the low-field region so that much more edge heating is expected than in future experiments. The diagnostics used for the experiment were the midplane diamagnetic loop, Langmuir probe, interferometer, and VUV monochromator. The forward and reflected power were also monitored.

Five different questions were asked:

1. How does the net energy absorbed change as the main magnetic field is changed?

2. How does the absorbed energy vary with injection power (for fixed RF pulse length)?

3. How does the net energy absorbed change with increasing RF pulse length (for fixed power)?

4. What is the variation of net energy absorbed with increasing line density?

5. What is the change in the bulk electron temperature, as measured with the Langmuir probe, due to the heating?

These questions were straightforward to answer experimentally and provided adequate demonstration of the operation of the magnetron.

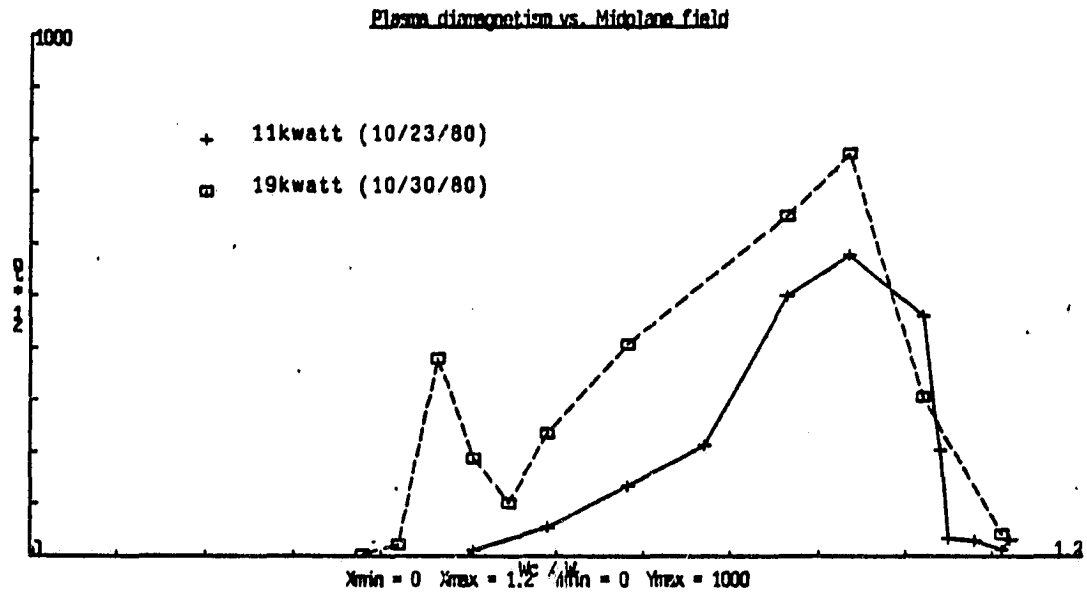

Figure 5.2. Peak changes in electron diamagnetism due to ECRH as the main magnetic field is varied. Without Ioffe bars. A first and second harmonic peak is observed.

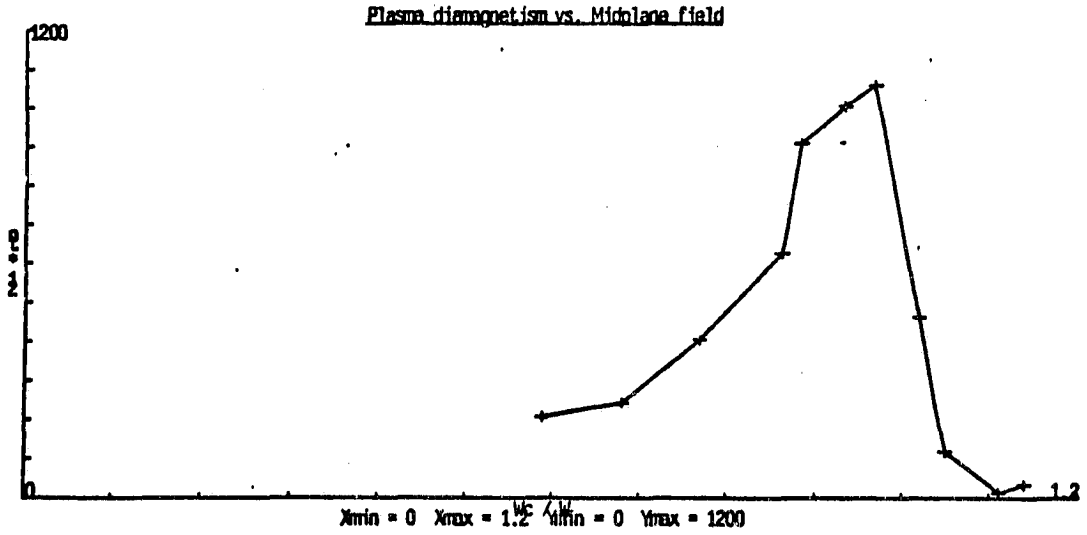

Figure 5.3. Peak changes in electron diamagnetism as the magnetic field is varied. With Ioffe bars.

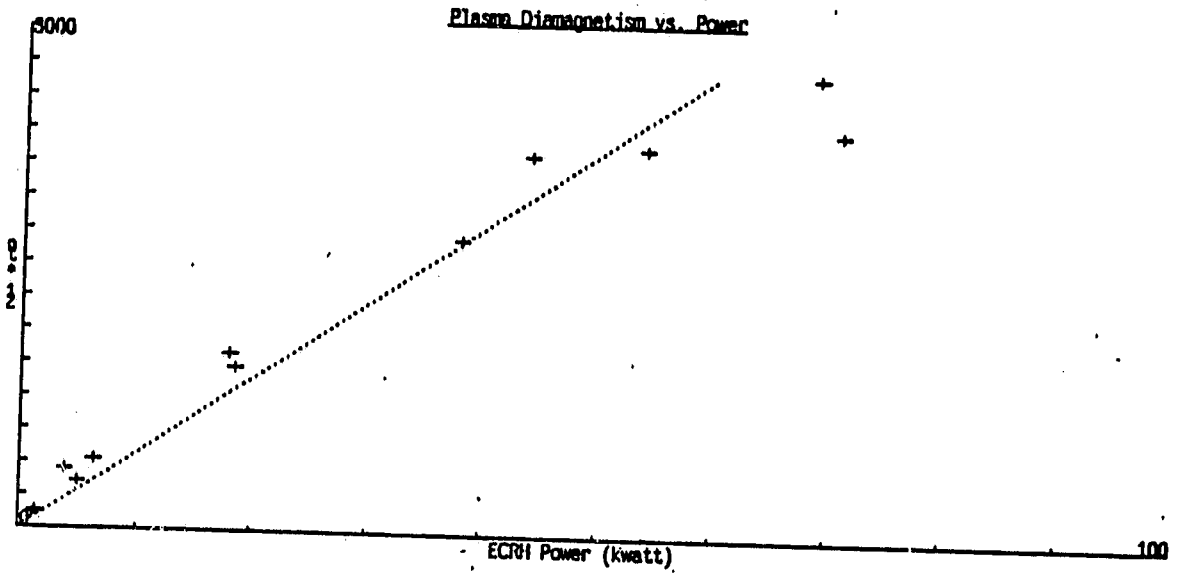

Figure 5.4. The peak change in diamagnetism vs. RF power for constant ECRH pulse length. Curve shows an approximate heating efficiency of 30%.

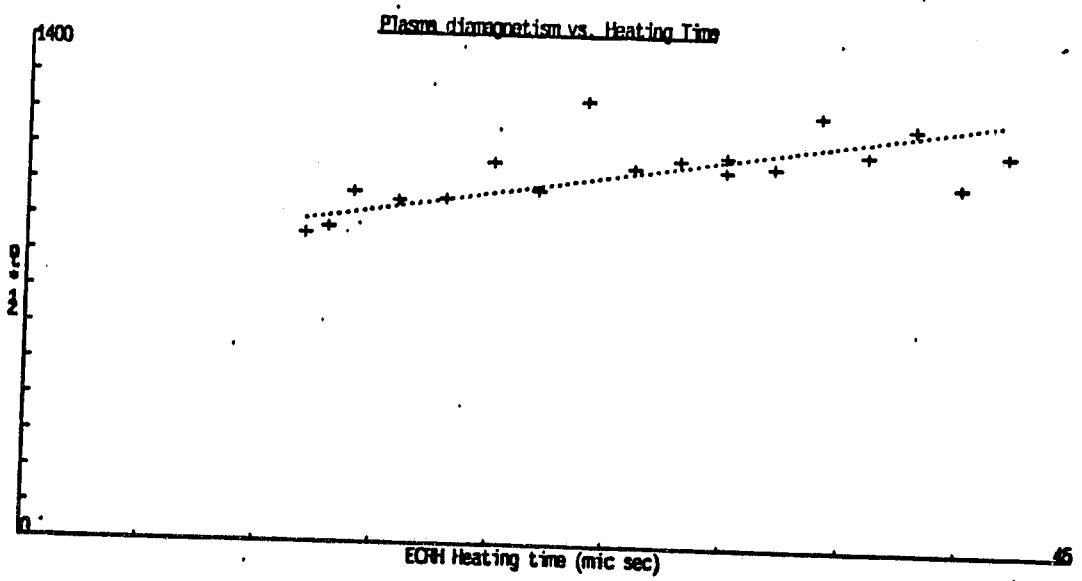

Figure 5.5. The peak change in diamagnetism vs. ECRH heating time for fixed power, 18kW. Comparison of this figure with Figure 5.4 indicates the slowing of the heating rate after the first $\lesssim 10\mu secs$.

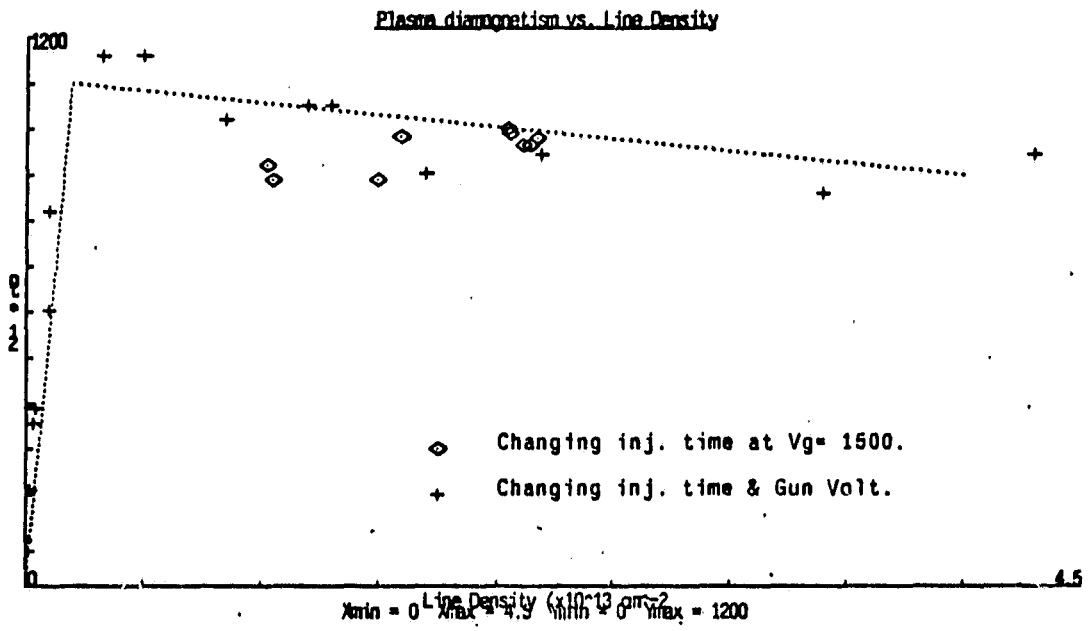

Figure 5.6. Changes in diamagnetism as the line density is varied.. With Ioffe bars. Notice the nearly constant net heating for densities above a very low threshold. The exact value of this low density threshold could not be measured. No high density cutoff was observed.

Figures 5.2 and 5.3 show the results of varying the magnetic field with and without Ioffe bars. Plotted on the graphs is the peak change in diamagnetism due to ECRH as the mirror field is varied from well below resonance to fields above which no resonance exists on axis. The addition of the Ioffe bars appears to sharpen the first harmonic resonance as compared to no Ioffe bar example. Also, second harmonic heating was observed without Ioffe bars. (No corresponding data are available when the Ioffe bars were energized since the Ioffe power supply cannot operate at low currents.) These data demonstrate resonance heating.

Figures 5.4 and 5.5 answer questions 2 and 3. The first shows a net heating efficiency of 30% for $20\mu sec$ RF injections and for RF powers up to $50kW$. This is approximately 5 times more efficient than that observed in Constance I [Ref. 25]. The second shows the net energy absorbed as the RF pulse is lengthened and reveals the very interesting result that, by $10\mu sec$, the heating and loss rates appear to have nearly equilibrated.

The change in the diamagnetism due to changes in density during heating is shown in Figures 5.6 and 5.7. The first figure represents the data when the Ioffe bars were energized, while the second is when the Ioffe bars were not used. Here, the density was controlled by lowering or raising the plasma gun voltage, and

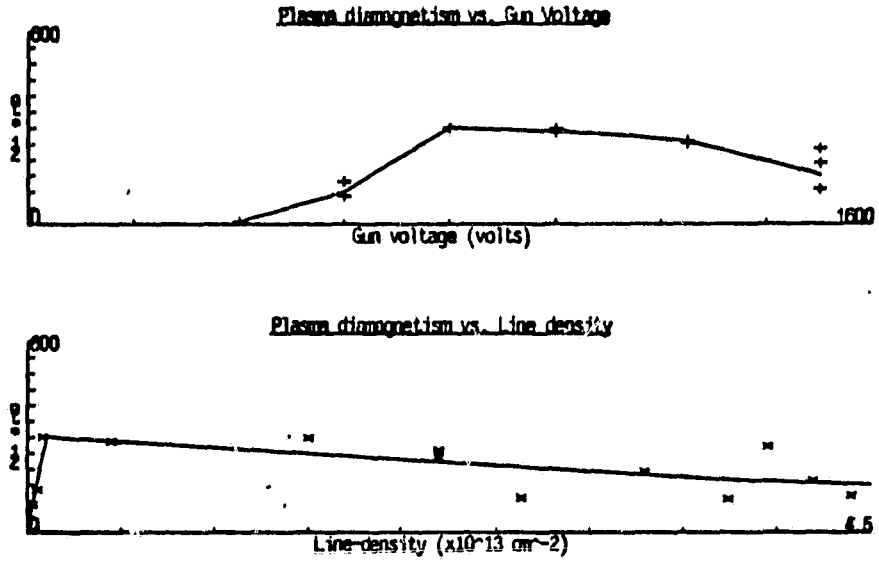

Figure 5.7. Changes in diamagnetism as the line density is varied. With no Ioffe bars. The top graph shows how this data was obtained: by varing the gun voltage. The general trends are the same as those shown in Figure 5.6.

the line density was monitored by the interferometer. In both cases, the maximum heating was observed at the lowest density that could be measured by the interferometer, although as the density increased no cutoff was observed. Whether this effect is due to the good accessibility of waves propagating along field lines or to edge heating will be determined with probes and Thompson scattering during future experiments.

Finally, the Langmuir probe data are shown in Figure 5.8, which plots the bulk electron temperature during and after the ECRH heating pulse for several injection powers. The peak bulk temperature increases by a factor of four from 5 to 20eV as the power is raised to 25kW. After the end of the RF, the bulk electron temperature returns to $\sim 5eV$ with a characteristic time of about $20\mu sec$. Figure 5.9 gives an example of the Langmuir probe data. The "bulk electron temperature" referred to here is found from the largest slope of the probe's IV characteristics. It was not possible to estimate the density or energy of an electron tail from these experiments.

Other data were taken in the course of answering the five "check-out" questions. The intensity of the oxygen VI impurity line was found to more than double during several $50kW$ heating pulses. After the end of the ECRH, the level decayed back to its normal level within a few tens of microseconds. The "hot electron instability" was observed under conditions similar to those found in Constance I by using the high impedance floating probe. A brief experiment was conducted to determine the effect of the ECRH on the

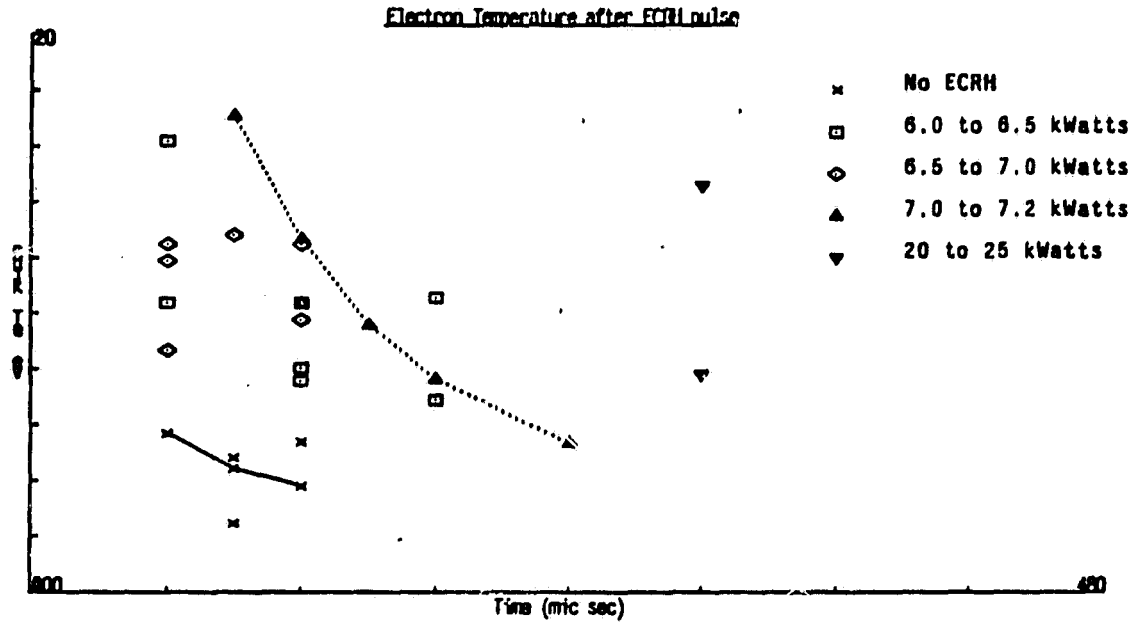

Figure 5.8. Several measurements of the bulk electron temperature during and after the ECRH pulse. Powers between 0 and 25kWatts were used. The heating started at $400\mu sec$ and lasted for $15\mu sec$. The temperature returns to its normal $\sim 5eV$ after about $20\mu sec$.

ion-cyclotron fluctuations observed at low densities. Although the fluctuation level was high and although, at high powers, the ECRH consistently reduced the fluctuations, the stabilization results were not repeatable at moderate and low powers. The data, representing 38 shots, are shown in Figure 5.10.

The build-up and decay times of the diamagnetic signals were recorded which can provide a useful diagnostic when their rates are compared to the classical collisional loss rates. Sample diamagnetic and interferometer data are shown in Figure 5.11 for two shots with and without ECRH. Notice the sharp ($\sim$ 1 to $5\mu sec$) increase in the plasma energy followed by the "equilibrium" maintained for the duration of the heating pulse. The energy decays to about 60% of the equilibrium value the instant the power is turned off and, then, more slowly ($\tau_{decay} \approx$ 20 to $30\mu sec$) for the remainder of the decay. The line density shows a remarkable increase during and a greatly slowed decay after the ECRH pulse. This may be due to edge heating or to turning-point accumulation.

Obviously, the many interrelated processes which give rise to the behavior observed here are complicated, and it is the purpose of future study to unravel them. However, a few simple calculations can suggest a course to follow.

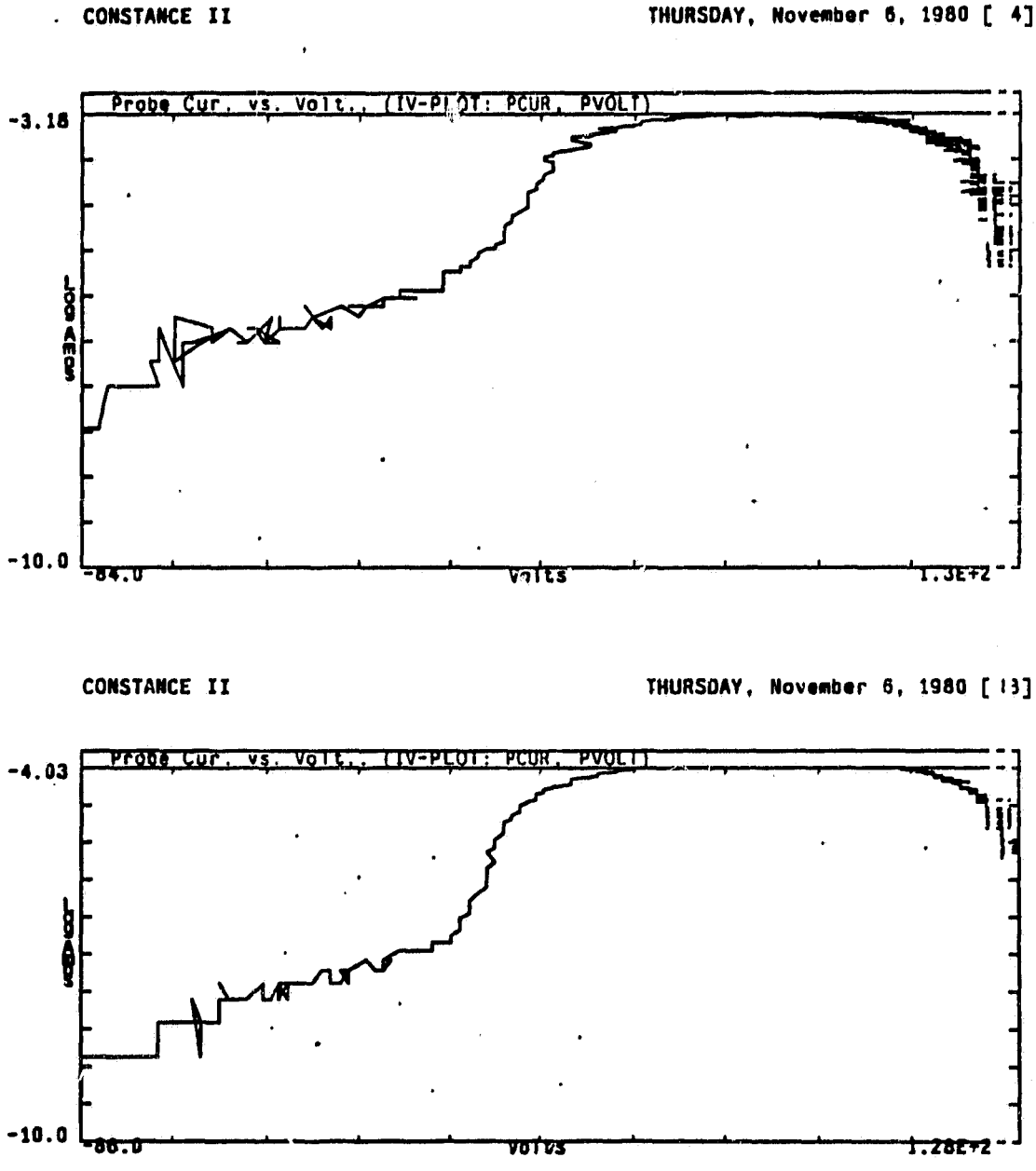

Figure 5.9. Example of the Langmuir probe data with (top) and without (bottom) electron heating. Notice the $\sim$ 3 times higher bulk electron temperature. The size or temperature of a warm electron tail could not be determined from this data.

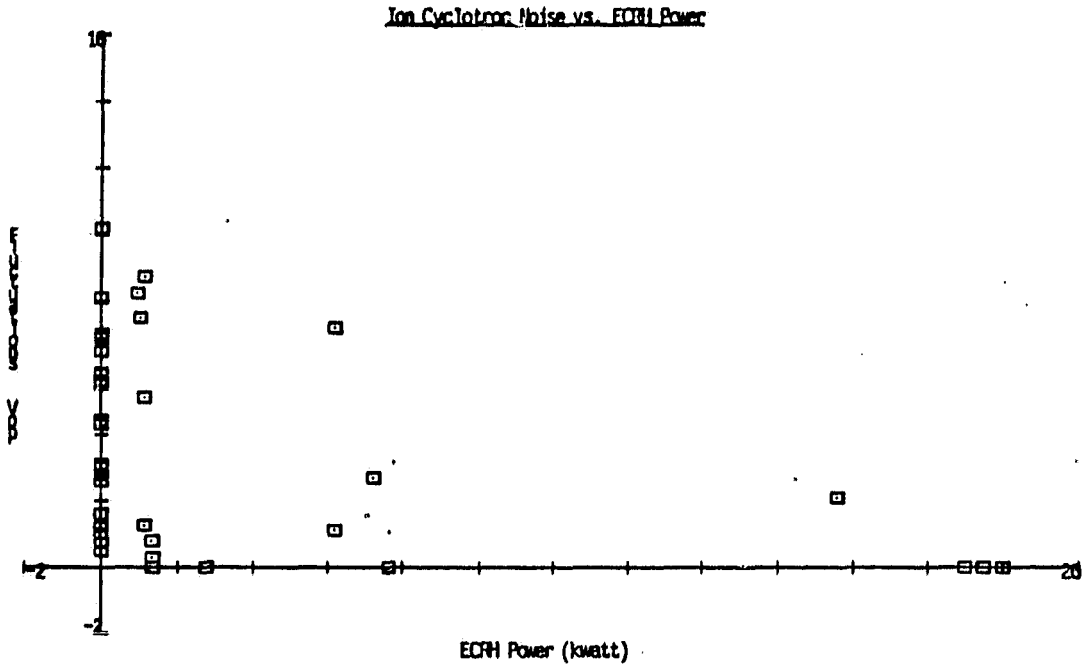

Figure 5.10. Results of 38 shots with and without ECRH while monitoring the ion cyclotron fluctuations in low density plasma. Titanium gettering was used before each shot. The results did not seem repeatable for low or moderate powers. More data will be taken at a later time.

The density during the RF pulse is between 0.5 and $1 \times 10^{13} cm^{-3}$, and the bulk electron temperature is 5eV. This corresponds to the "long injection" mode of operation described in the section on confinement studies. The diamagnetic measurement, therefore, gives the ion temperature to be between 15 and 35eV. The, then the $6kW$ heating pulse is applied, nT climbs by $400 \times 10^{12} eV cm^{-3}$ even though the bulk electron temperature only rises by 15eV. Since the Langmuir probe data do not exclude the possibility of a 10-15% hot electron tail, the data are self-consistent (assuming no complications due to edge heating) only when there is a tail of energy between 250 and 700eV. Furthermore, the total decay time (collisional plus drag) for 500eV electrons in a $5 \times 10^{12} cm^{-3}$ cold plasma is $20 \mu sec$. (These are the same arguments used by Mauel, [Ref. 25] to suggest that "warm" not "hot" electrons were responsible for the observed DCLC stabilization). Finally, $5kW$ is equal to the power loss of a half-liter plasma at $2 \times 10^{12} cm^{-3}$ containing 500eV electrons with an energy confinement time of $20 \mu sec$. Thus, the balance of the observed energy loss rate and input RF power is "close enough" to indicate that the observed ECRH equilibrium is plausible.

Plasma Gun Studies

1. Introduction .

The hot ion plasmas in the Constance II mirror experiments are produced by plasma guns of the washer type. Most of our experiments utilized the Ti washer gun developed by Coensgen [Ref. 6]. (I) With gun discharge currents in the 1000 amp range, and durations of 300-500 μsec. The plasma injected into the mirror region has a significant hot ion component ($T_i \gtrsim 100 - 150eV$), and an essentially cold component. At "low" densities $10^{11-12} cm^{-3}$, the ions are mostly hot. At higher densities there is a mixture of hot and cold ions. The neutral gas injected into the mirror remains below 5×10^{-6} Torr for about $1msec$. This is a remarkably simple system for producing an "interesting" plasma. Unfortunately, there is no independent control over density or temperature. Thus, we have been studying some of the detailed characteristics of the Ti washer gun in order to better understand how it works; and we have investigated some washer guns in which the Ti washer was replaced as an H_2 source by a pulsed gas valve.

The 2" Ti washer gun that we obtained from Lawrence Livermore Lab is shown in Figure 6.1. Our modified pulsed gas gun is shown in Figure 6.2. The Ti anode has been replaced by Mo. The gas valve opens and closes in about 2 msec. A similar gun with a 1/2" dia. cathode and anode is now being studied in Constance II.

The pulsed gas gun was built to test the observation that the ion temperature varies inversely with the gas density in the gun. The gas valve would allow us to independently control the gas density. This has turned out to be only partly true. There is a reservoir of gas on the surface of the cathode and the other electrodes that establishes the minimum gas density during the discharge. However, the valve gun does not have the run-away pressure build up at long pulses that accompanies the heating of the Ti washer, and preliminary observations indicate that levels of metallic impurities are much reduced in the valve gun.

The mechanism responsible for heating the ions is still a mystery. During the gun discharge, the anode-cathode voltage lies in the range 100-200 volts. Nevertheless, we observe ions with energies of 1000eV, or more. This indicates some sort of cumulative acceleration - either by a coherent wave interaction or by a stochastic process.

The mechanism responsible for heating the ions is still a mystery. We observe ions with energies out to 1000eV, or more, and we believe that they are accelerated by some cummulative process - either by a coherent wave interaction of by a stochastic (turbulent) process. Our initial assumption was that we would

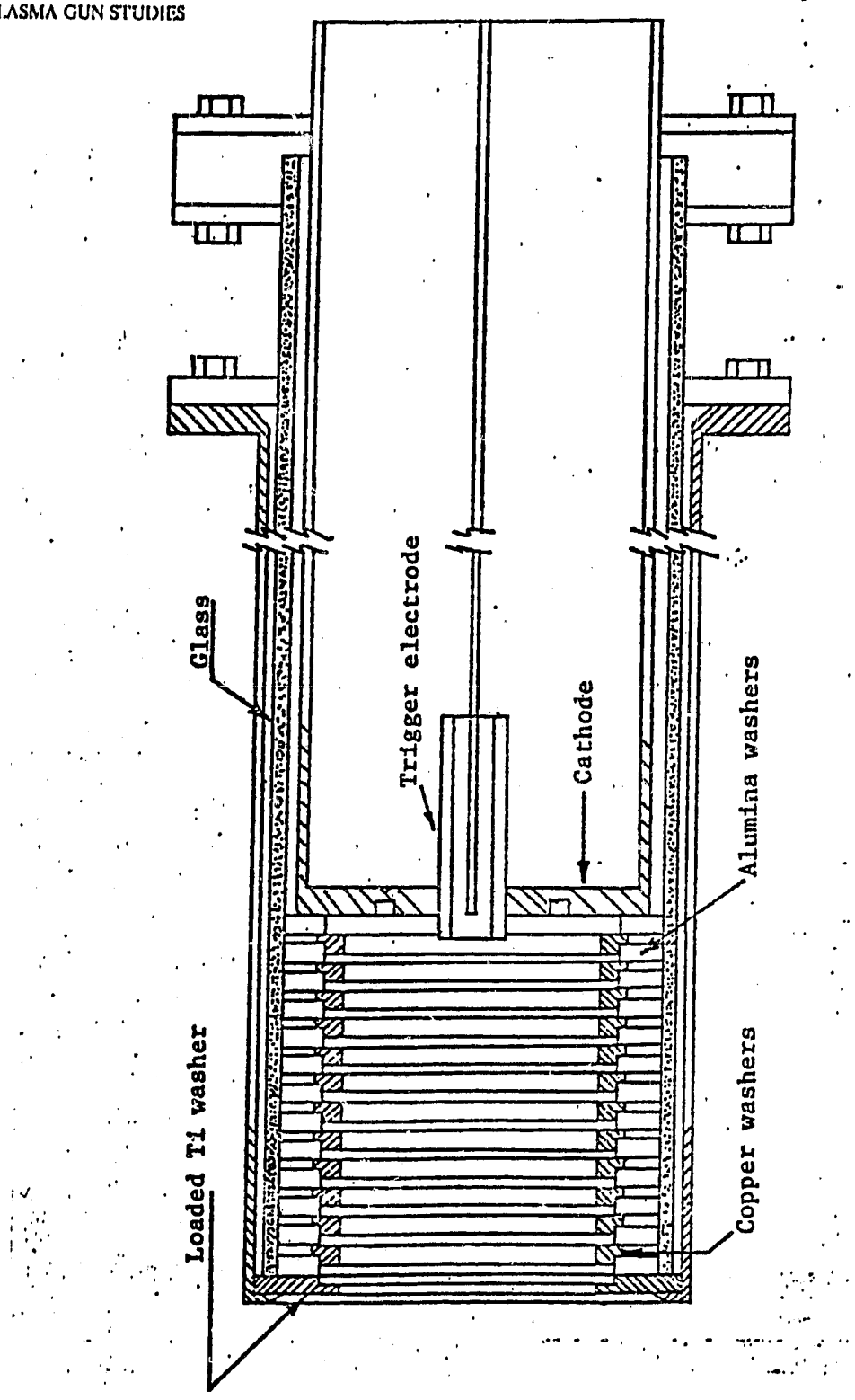

Figure 6.1. Schematic of Ti washer gun. From LLL.

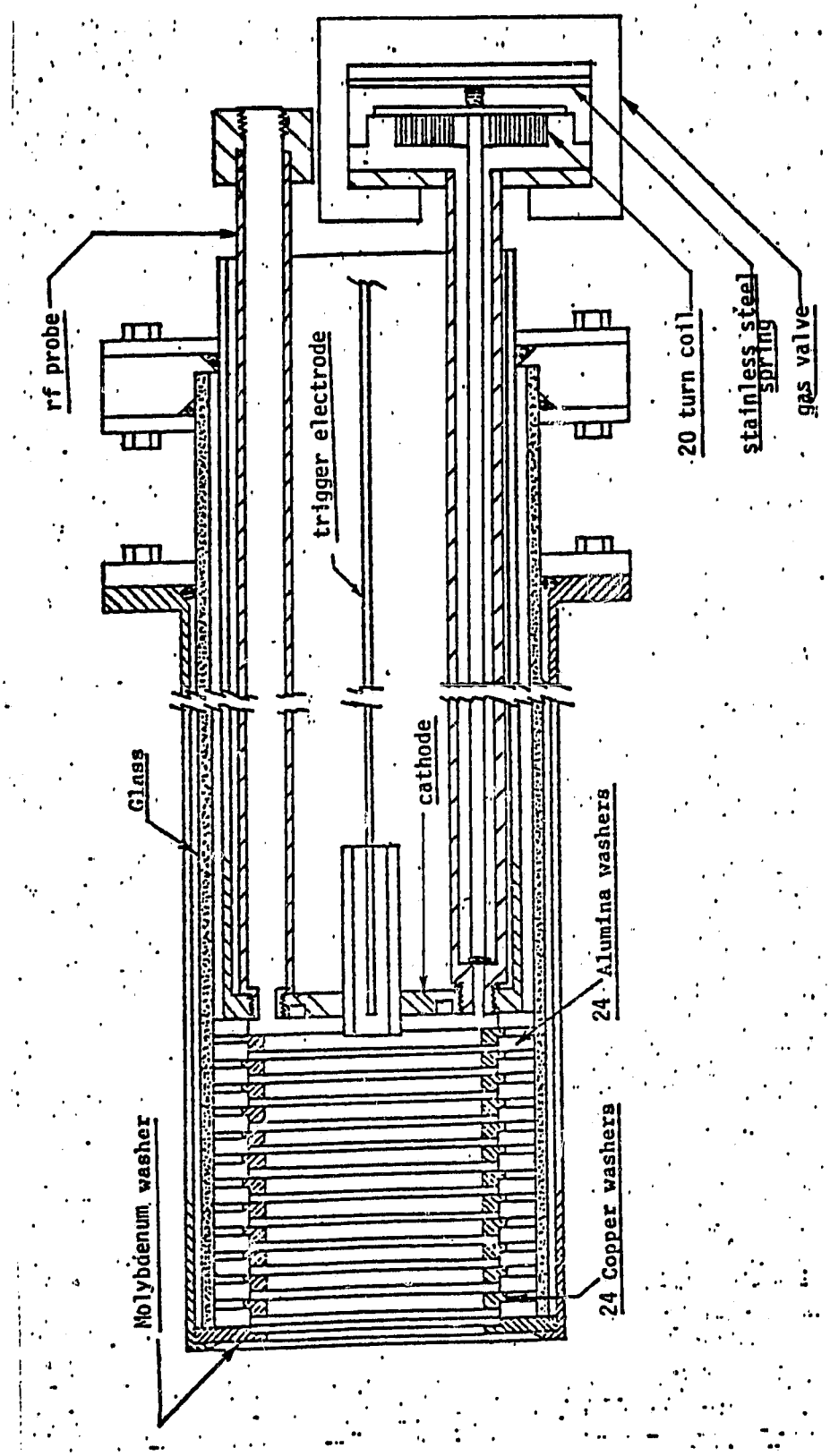

Figure 6.2. Schematic of pulsed gas gun.

find a strong oscillation at f_{pe} driven by the electron beam plasma interaction near the cathode. A lengthy search has failed to detect the expected mm wave signals, or any strong signals $\gtrsim 1.5GHz$. However, there is a strong band of signals in the neighborhood of 1 GHz, which is close to the ion plasma frequency. These oscillations may be responsible for the ion heating, but we still do not know how they are excited or energized.

2. Gun Measurements .

The work reported here follows on that of Rymer [Ref. 40], and is somewhat parallel to that of Osher. [Ref. 33]. We present here a sampling of some of the measurements made in the plasma stream leaving the gun.

The guns tested were 2" washer guns - Ti-washer and pulsed-gas. They were excited by a delay line with an internal resistance of about 0.5 ohm. Since the effective arc resistance was about 0.1 ohm, the system was nearly constant current controlled by the bank voltage. The principal measurements made on the plasma stream launched by the gun were:

- Stream current I_s (Rogowski coil, collector plate)
- Total energy (flat plate calorimeter)
- Diamagnetism, $W_\perp$
- Visible spectrum
- Radio spectrum

The important adjustable parameters were

- Pulser bank voltage, V_b
- Guide field strength, B_g
- Injected gas, controlled by the valve voltage V_v

A 2" pulsed gas gun was installed in Constance II, and fired with various valve settings. The pressure rise in the 500 liter tank was measured with the pumps valved off. Figure 6.3 shows the relation between injected gas pressure and valve voltage. It is evident that the gun produces a plasma with no injected gas

($V_v = 0$), and that the valve only adds gas above the minimum levels indicated. The ambient pressure was about $5 \times 10^{-7} T$, and the time between shots was minutes, so that there was ample time to absorb the amount of gas evolved. The cathode area of 20 cm^2 could easily contain more than 10^{16} molecules, and a similar number is available from the inner surfaces of the washer stack. One conclusion we may draw, is that the Ti washer's function is to load the electrode surface with H_2 for the succeeding shot!

For the subsequent data reported here, we used a somewhat improved valve. Its calibration, of injected molecules vs valve voltage is shown in Figure 6.4.

The stream current, $I_s = I_- - I_+$ was a net electronic current for all the range of parameters we observed. It's dependence on B_g is shown in Figure 6.5. The dependence on gun voltage is shown in Figure 6.6. Figure 6.7 shows the time dependence of the stream current of the pulsed gas gun. The rise in current at the end, we believe, corresponds to a depletion of gas in the gun, (see Figure 6.10).

Figures 6.8 and 6.9 show the dependence of diamagnetism, $W_\perp$, with bank voltage, and magnetic field strength.

Figure 6.10 shows the effect of injected gas on: stream current, diamagnetism, and total energy. The increasing diamagnetism with iV_v represents a denser but cooler plasma. Figure 6.11 shows the variation of $W_\perp$ with bank voltage for several levels of injected gas.

The visible spectrum signals of some impurities (Cu, Fe, and Mo) are shown in Figure 6.12 for the pulsed gas gun, for the cases of injected gas and for no injected gas. It is apparent that the impurity signals are greatly reduced with injected gas. We have observed that guns operated with no injected gas show signs of melting around the anode aperture, and on some of the copper washers.

We explored the RF spectrum of the fluctuations in the plasma stream, and to a limited extent within the gun itself. Except for the first few microseconds of the discharge, we have not been able to detect signals above about 1-1.5 GHz. With plasma densities greater than 10^{13}, we would have expected plasma frequencies in the range above 30 GHz. We did, however, find a relatively strong band of frequencies in the range 500-1000 MHz; this corresponds, roughly, to the ion plasma frequency.

Figure 6.13 shows the rectified signal picked up by a probe and filtered by a 200 MHz high pass filter, also shown is the gun voltage. It is generally observed that the rf signal goes to zero when the gun voltage falls below a critical value, usually 150 volts. In Figure 6.14 the behavior of the rf is shown for various bank voltages, and it is evident that the rf lasts longest for the lowest voltages, the time to cut off always corresponding to the same critical gun voltage. In Figure 6.15 we show the effect of introducing more gas, and we see that the time to rf cut off and to the critical gun voltage decrease together. These observations correspond to results on Ti washer guns in Constance II, that show hot ions being produced during the early part of the pulse, and lasting longer for lower bank voltages.

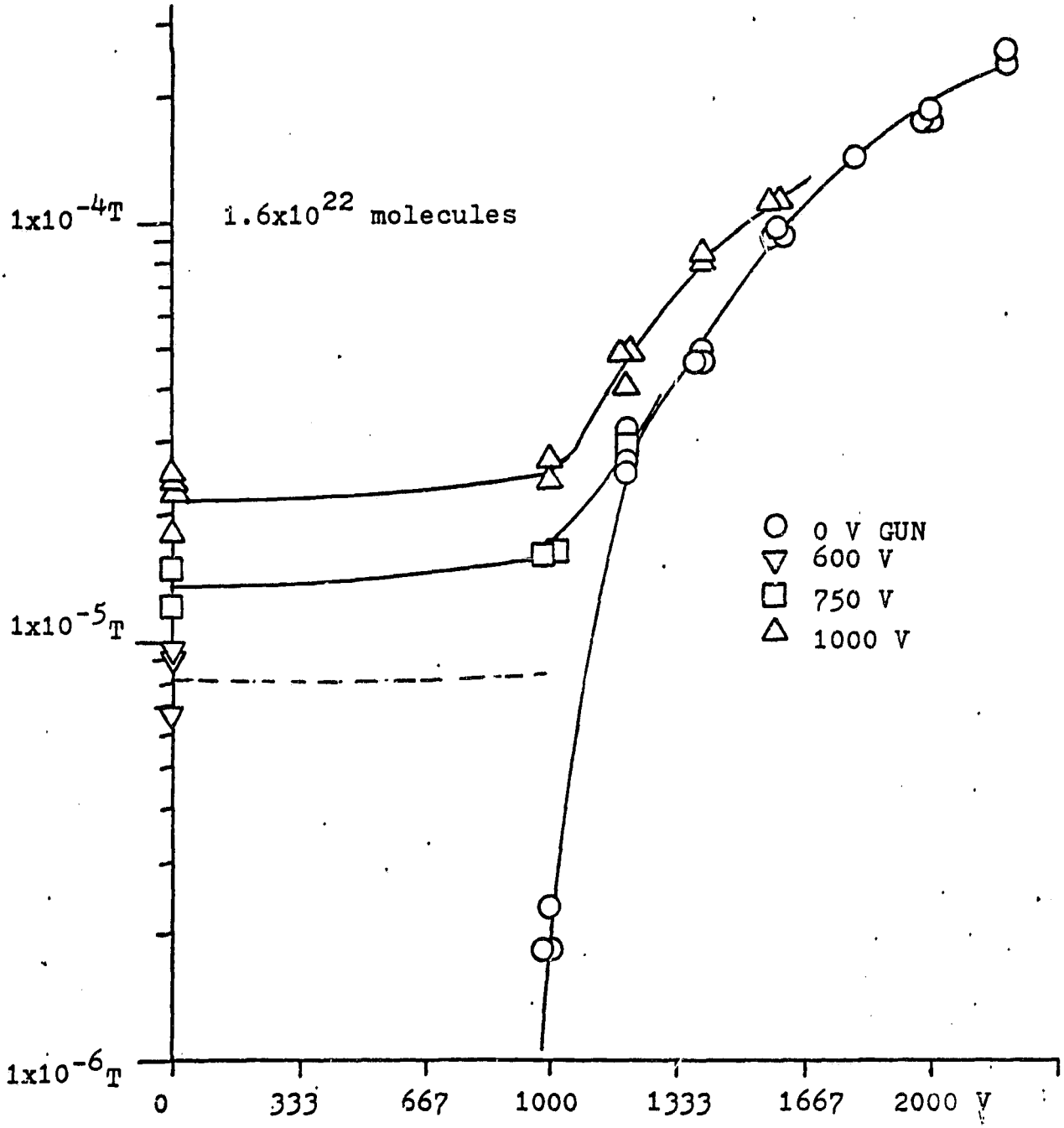

Figure 6.3. Injected gas pressure vs. valve voltage.

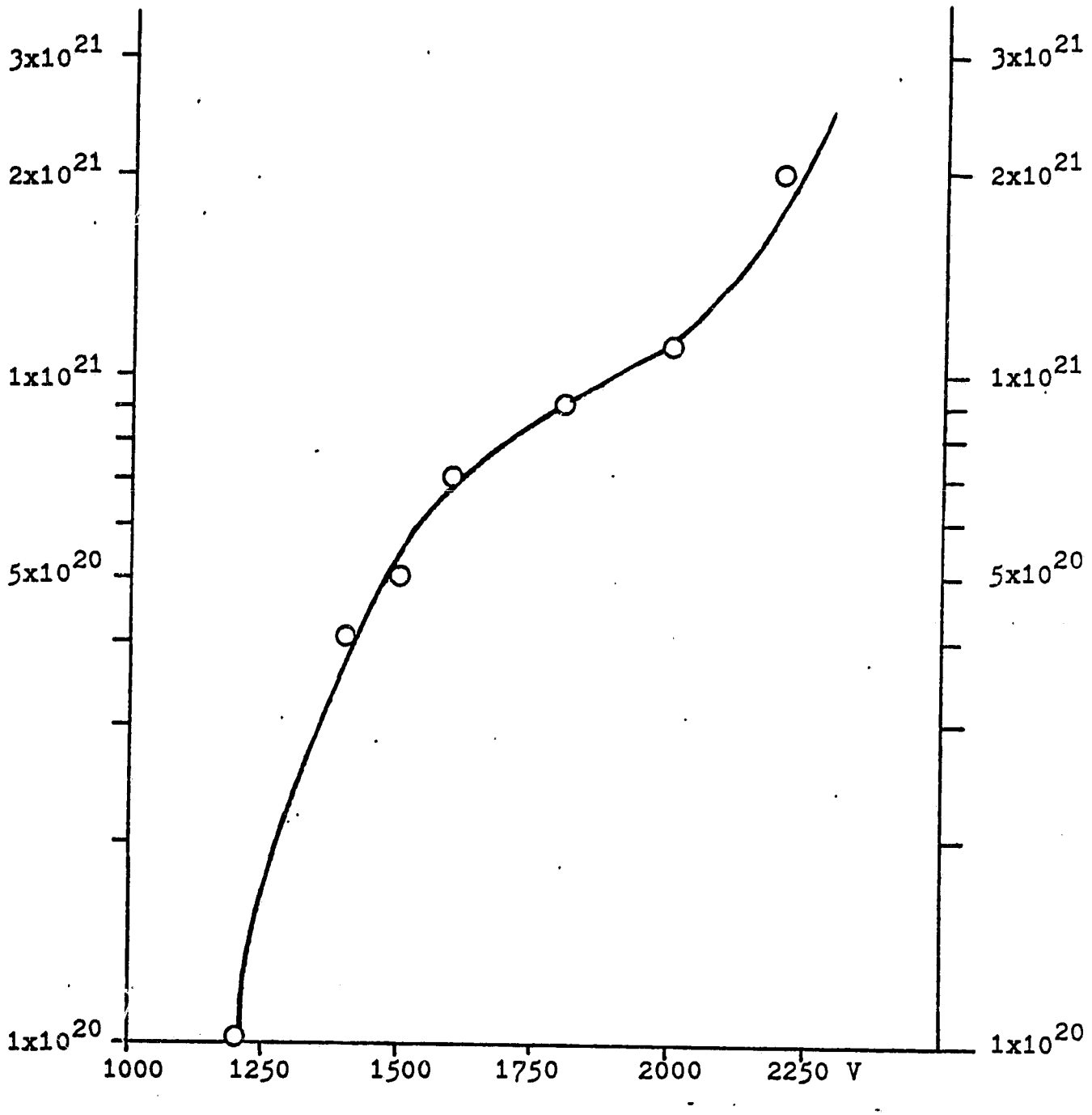

Figure 6.4. Number of injected molecules vs. valve voltage for improved valve.

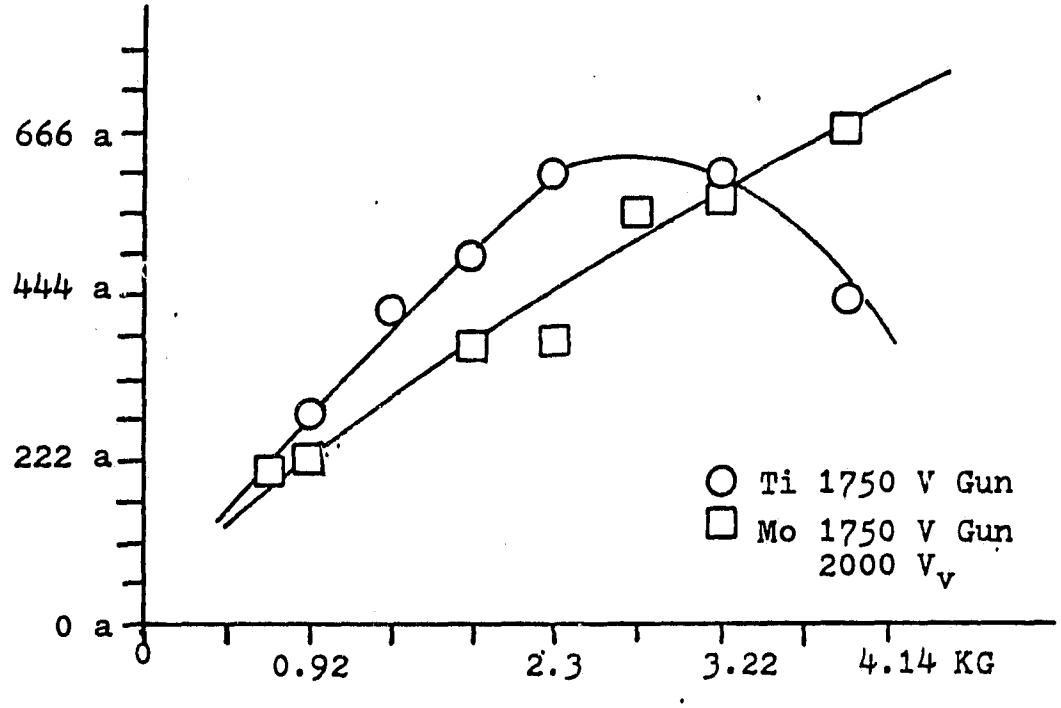

Figure 6.5. Dependence of stream current vs. guide-field magnetic field.

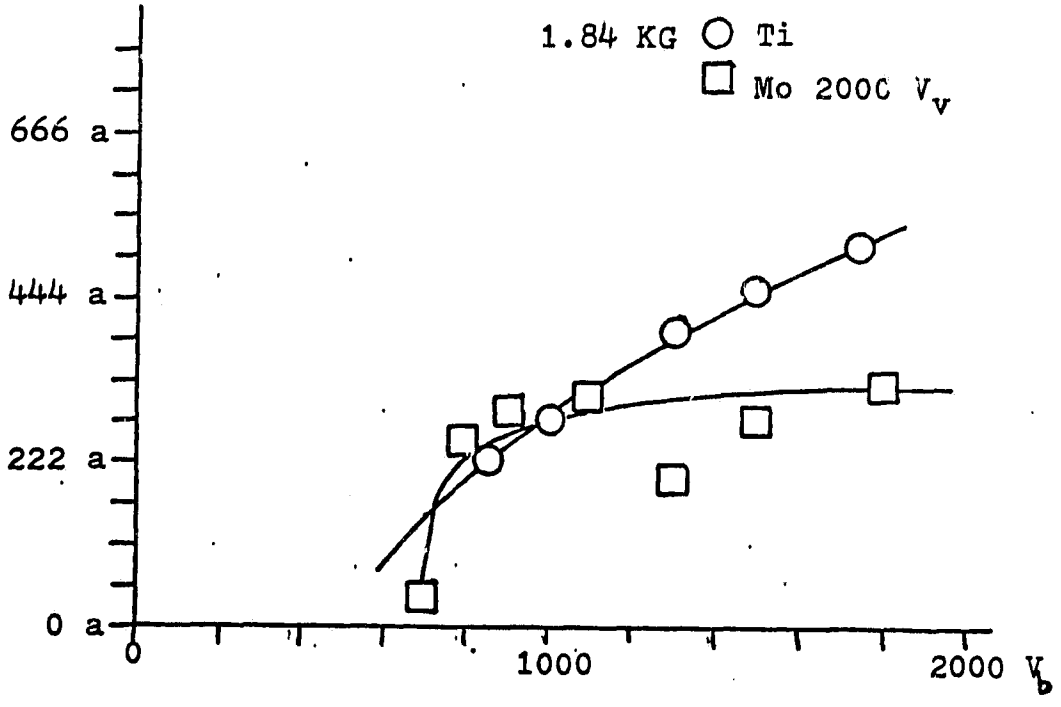

Figure 6.6. Dependence of stream current vs. gun voltage.

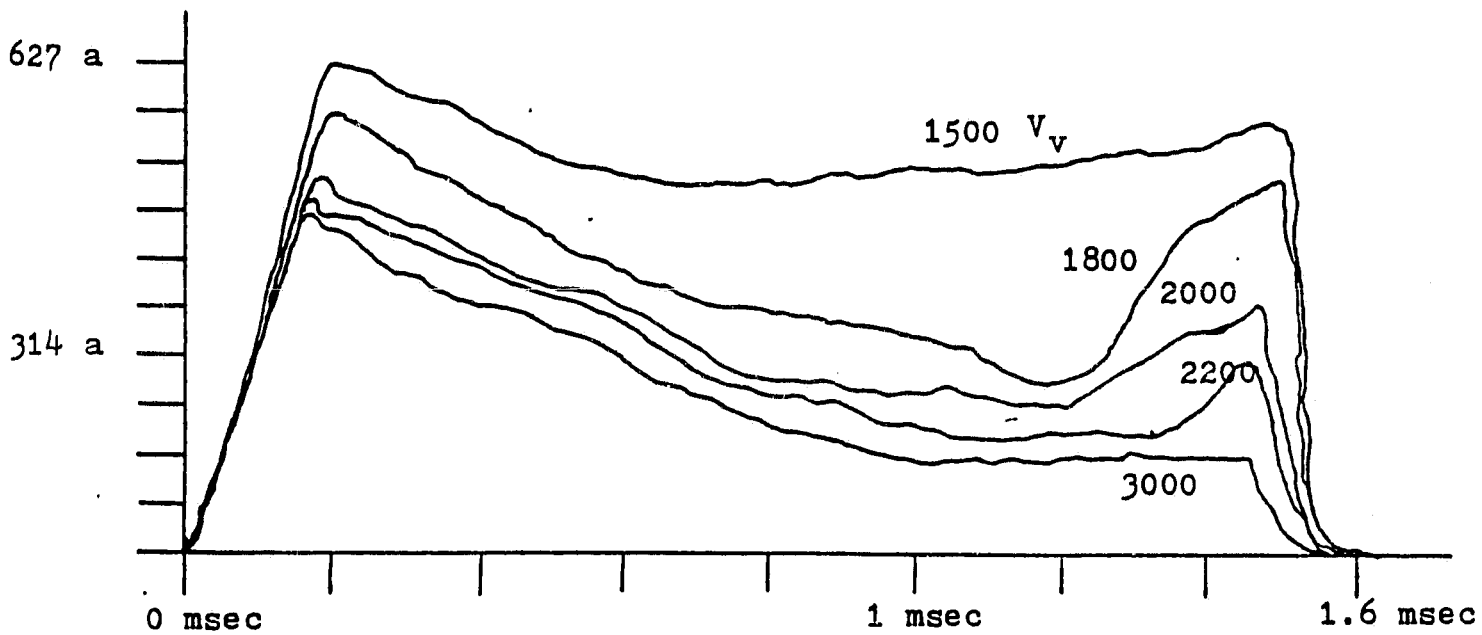

Figure 6.7. Time dependence of stream current for the pulsed gas gun.

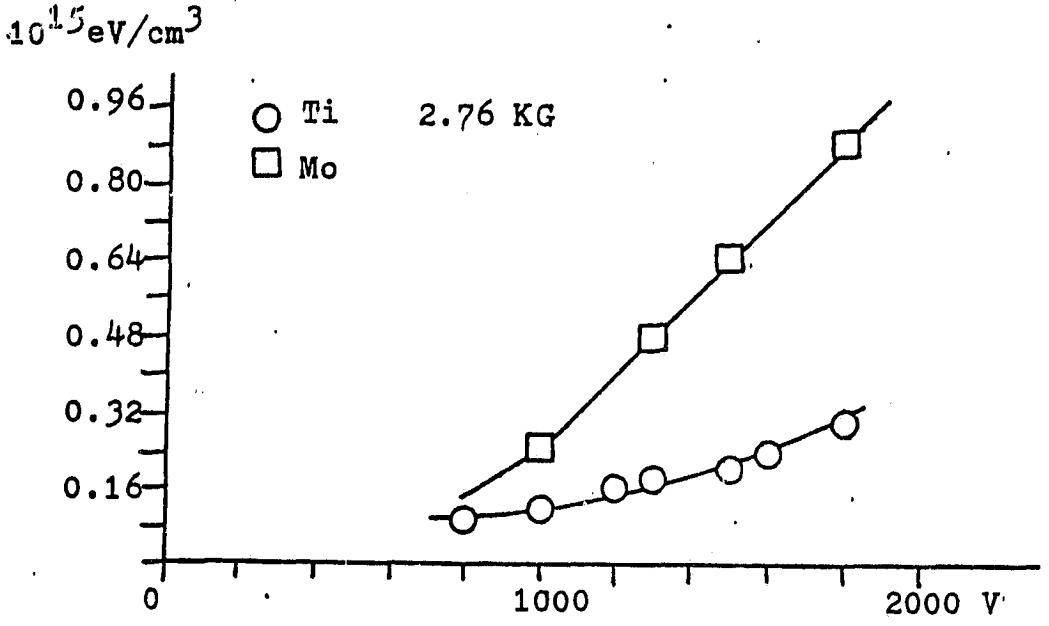

Figure 6.8. Variation of diamagnetism and $W_\perp$ with bank voltage.

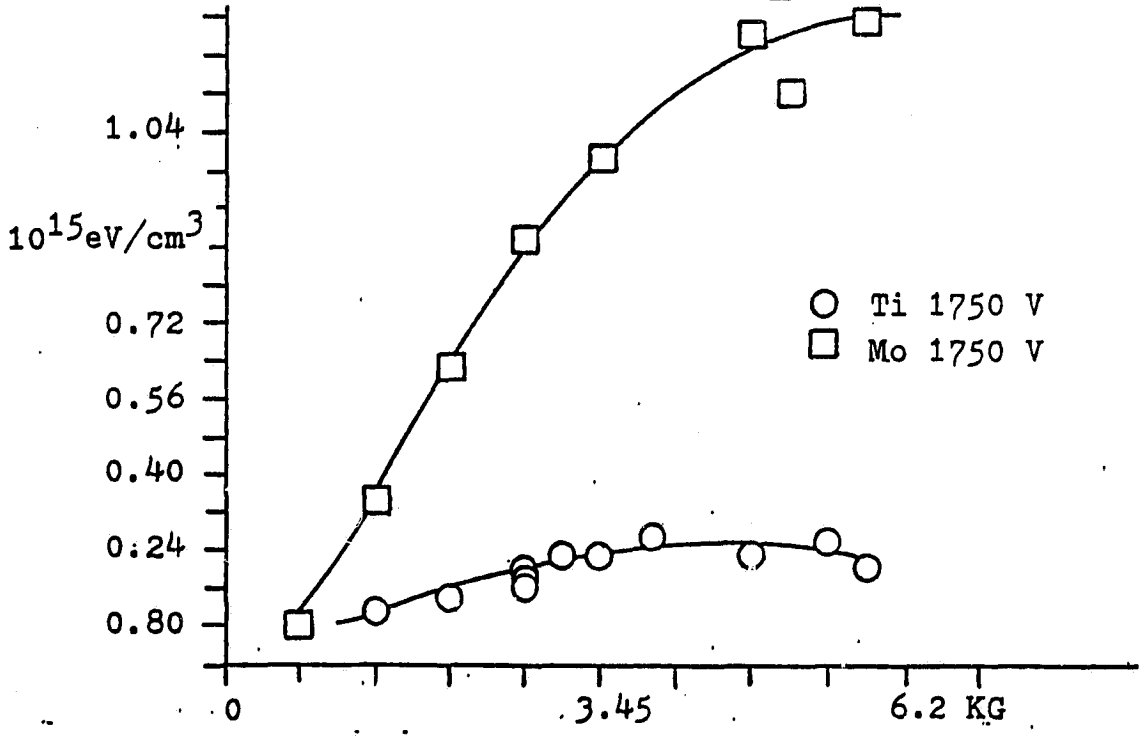

Figure 6.9. Variation of diamagnetism and $W_\perp$ on magnetic field strength.

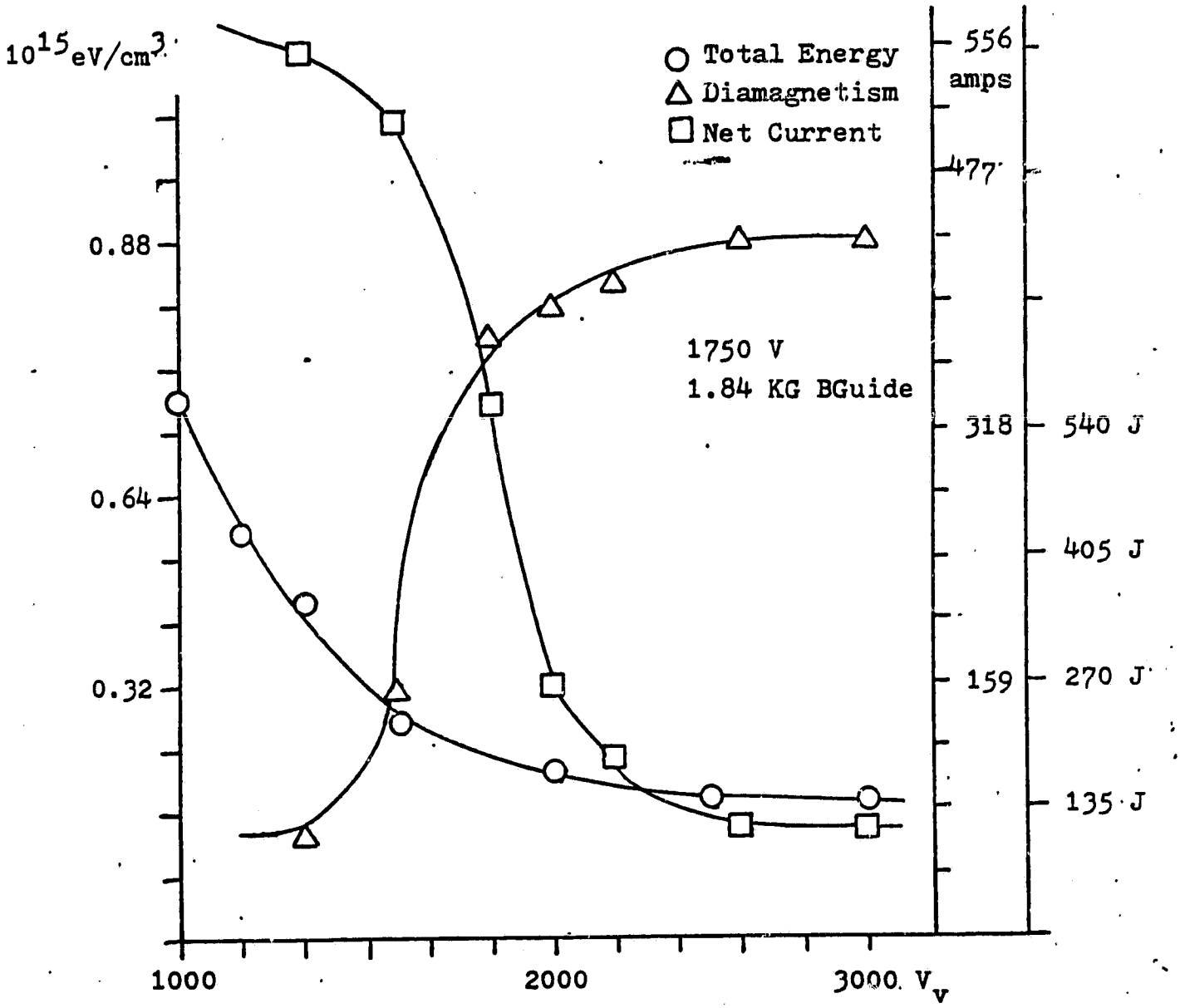

Figure 6.10. The effect of injected gas on the steam current, diamagnetism, and total energy.

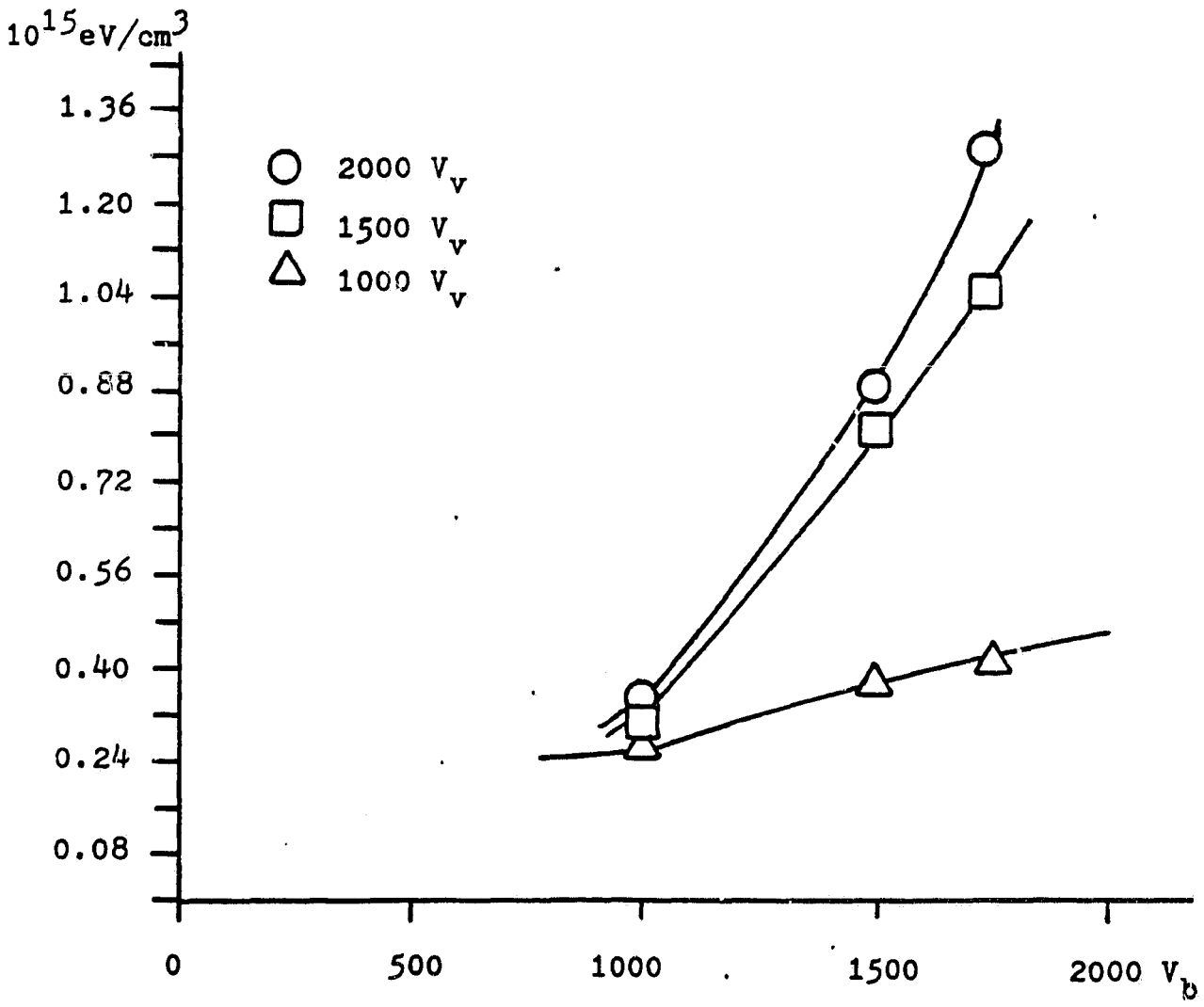

Figure 6.11. The variation of diamagnetism as the bank voltage is changed for several levels of injected gas.

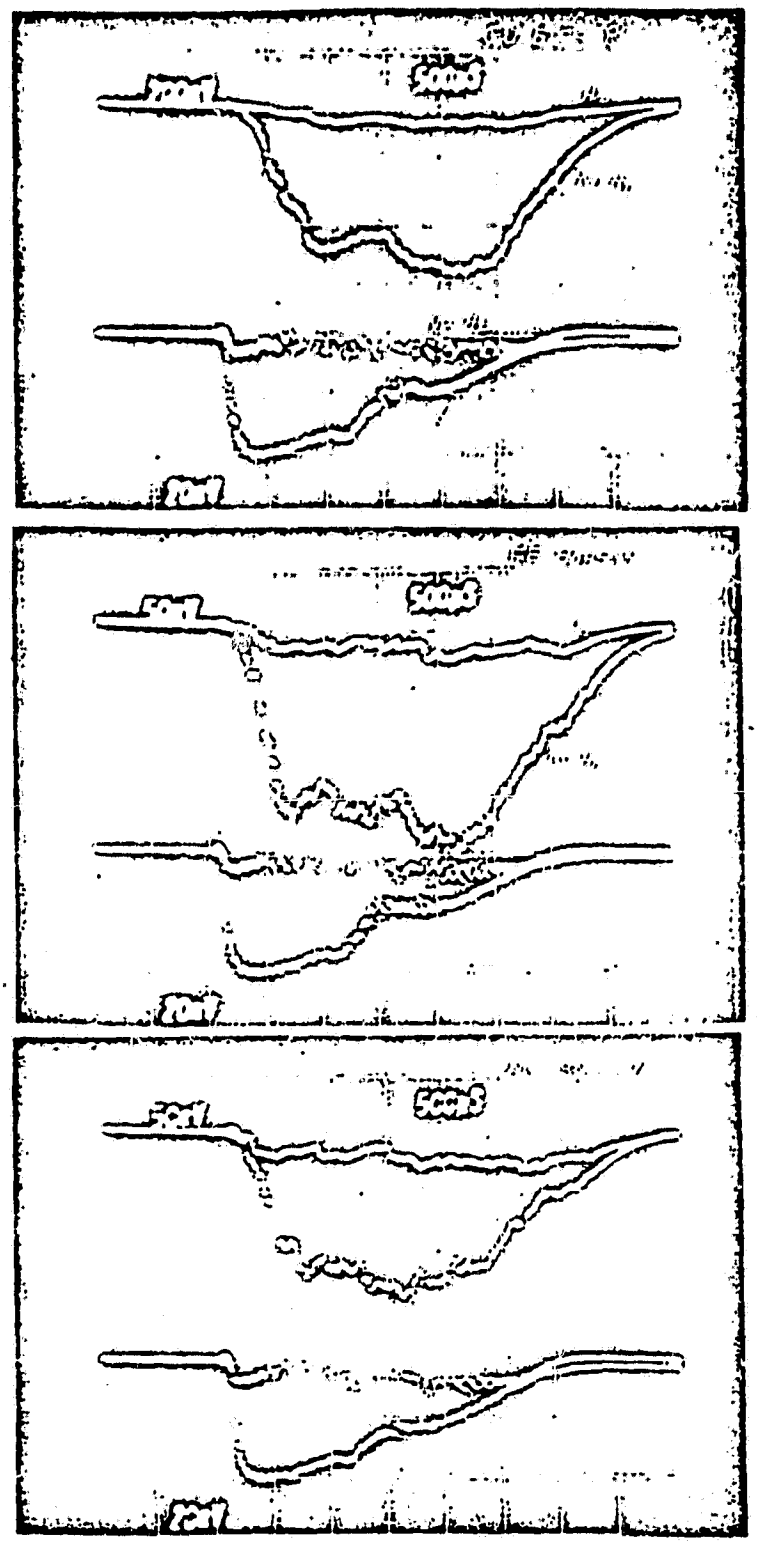

Figure 6.12. A comparison of the impurity signals of Cu, Fe, and Mo with and with out injected gas.

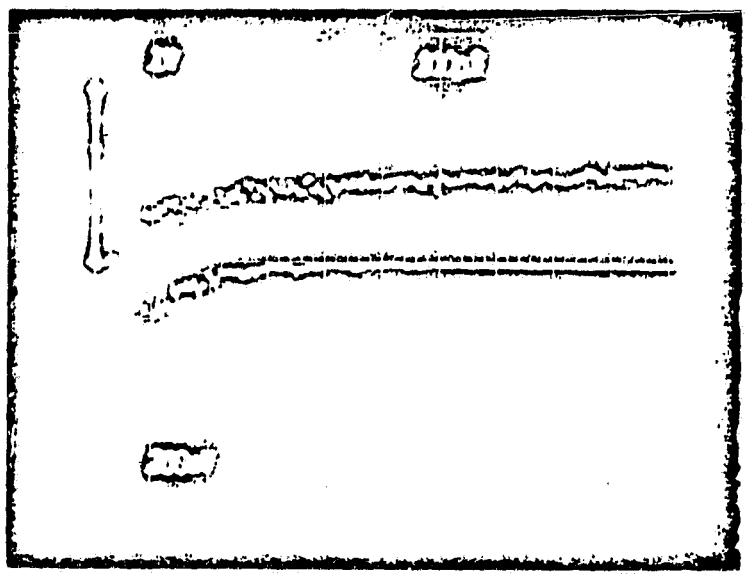

Figure 6.13. Rectified signal of the RF after a 200MHz high pass filter.

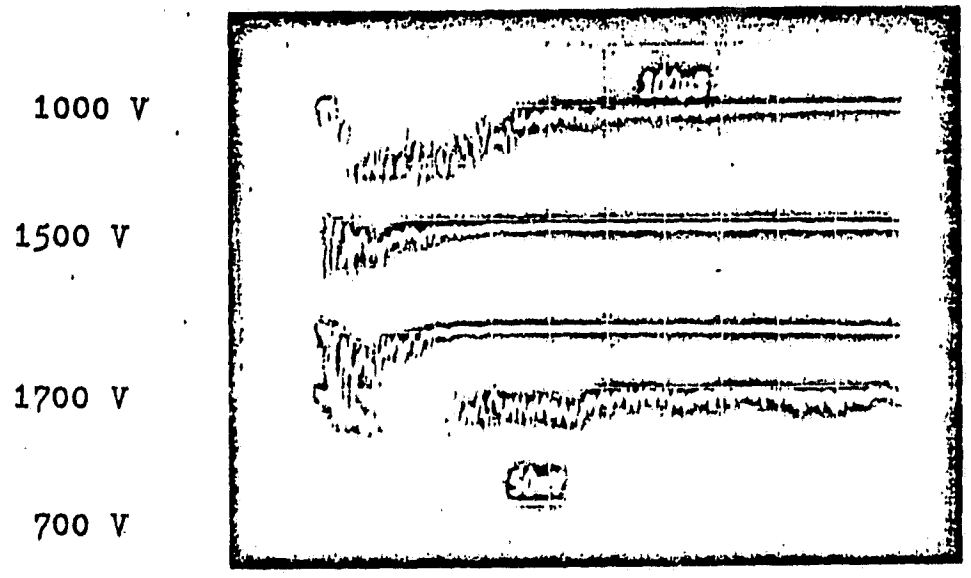

Figure 6.14. Behavior of RF as bank voltage is changed.

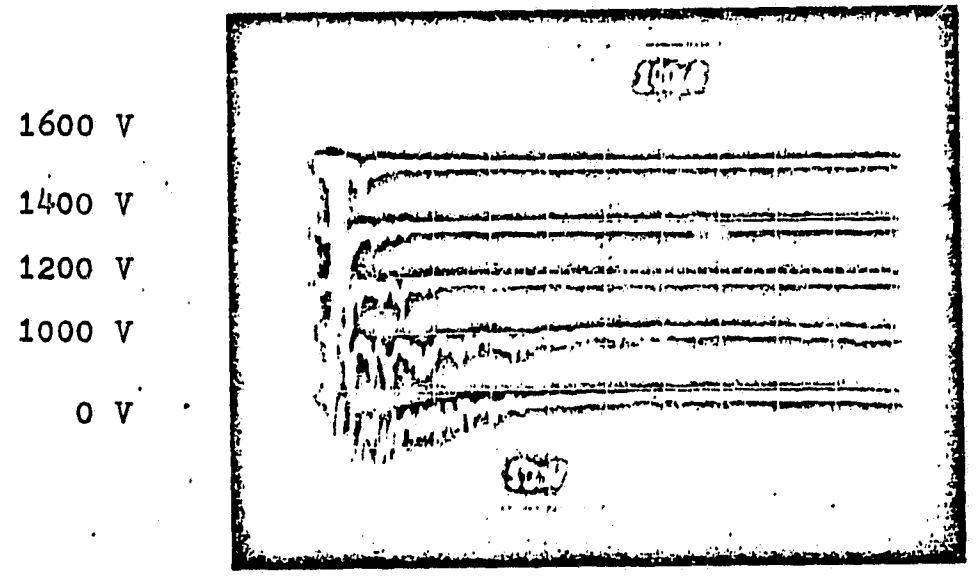

Figure 6.15. Effect of adding more gas.

3. Discharge Mechanism .

In this section we consider a model of the "steady state" discharge in the washer gun. We know that the discharge current I_D is constant at, say, 1000 amps with an anode-cathode voltage $V_S \simeq 100-150$ volts. Visually, the discharge seems uniform over the whole cathode and there are no pit marks on the cathode to indicate arcing. If we assume that all of the discharge power (100kW) is dissipated at the cathode ($20cm^2$), the temperature rise of a copper slab after 1 msec is $\sim 100^\circ C$(4), thus thermionic electron emission is excluded. The discharge current $I_D = I_+ + I_e = I_+(1+\gamma)$ where I_+ is the ion current and γ is the secondary emission of electrons by ion bombardment. For clean Cu (no gas layer), $\gamma \approx .01$.(5) However, for a gas covered target $\gamma = 0.1 - 0.2$.(6) Let us assume $\gamma = 0.2$. Then $J_+ \simeq 40a/cm^2$. Let us assume T_e in the discharge plasma $\simeq 20eV$, then we compute $n \simeq 4 \times 10^{13}$. We know that outside the gun, an 8mm interferometer is cutoff, $n > 1.7 \times 10^{13}$. Thus the model seems to hold, so far. In the "steady state", the ions flowing to the cathode must be replaced. Since excitation cross sections are about equal to the ionization cross section, we assume an "effective" ionization energy $V_i' \simeq 30$. The power needed to sustain the ion flow is $P_i = I_+ V_i' \simeq 24kW$. The power source is assumed to be the secondary electrons $I_e = \gamma I_+$, accelerated by V_D, $P_e = 0.2I_+ \times 150 = 30I_+ = 24Kw$. This is a little too close for comfort, but it is plausible!

The ionization is due to the primary electrons and the plasma electrons. If the neutral density is $3 \times 10^{14}(10millitorr)$, the primary electrons have a mean ionization path $\simeq 30$ cm, much longer than the gun. However, if $T_e = 20eV$ for the plasma ($n = 3 \times 10^{13}$) electrons, $< \sigma v >_i \simeq 1.1 \times 10^{-8}$ and the ionization rate can be accounted for within the gun structure ($L \approx 8cm$). The transfer of the primary beam energy to plasma electron energy could be accounted for by the beam-plasma interaction (Langmuir's famous paradox). This requires the excitation of a strong ω_{pe} oscillation ($f_p \simeq 56GHz$) in a layer just beyond the cathode fall. We have not yet been able to detect such oscillations and it is not clear if the failure is due to measuring techniques or if there really are no such oscillations. If there were such strong oscillations then they could set up modulational instabilities and generate the oscillations that we do observe at ~1 GHz which is about f_{pi}.(7) Alternatively, there is the model of Coppi's [Ref. 8] based on a "slide away distribution" that predicts the direct excitation of f_{pi} oscillations without any f_{pe}. These questions are being studied now.

4. Hot Cathode Plasma Gun .

In addition to our studies of pulsed gas washer guns, we have begun the construction of a hot-cathode plasma gun similar to those used by Nezlin [Ref. 30] and Ioffe [Ref. 17, 18]. The reported performance of these guns seems to exceed that of the washer gun. However, there is not much detailed description available in the literature. The apparent advantage of this gun is that it gives us one more degree of control by virtue of having a thermionic cathode (LaB_6) so that the ratio of electron to ion current at the cathode may be increased. Since the cathode runs hot ($> 1500^\circ C$), there will be no reservoir of surface absorbed gas as in the cold cathode washer gun, and the amount of gas in the discharge will be more fully

controllable by the gas valve. The principal technical problem has been that of designing a long lived W filament to heat the graphite - LaB_6, 2 cm dia. cathode. This seems to be solved, and we are proceeding with the construction of an assembly for Constance II.

5. Technology .

5.a. Fast Gas Valve. . An electromagnetic gas valve has been built that has an open time of about 300 microseconds. With a fore-pressure of 1 atmosphere of H_2, it can inject up to 1.5×10^{18} molecules into a vacuum system. The valve is activated by the discharge of a 3 uf capacitor (2-3kv) into the coil. Figure 6.16 is a sketch of the device, and Figure 6.17 shows the pressure transient measured 15 cm away from the valve nozzle, in the 500 liter Constance II chamber.

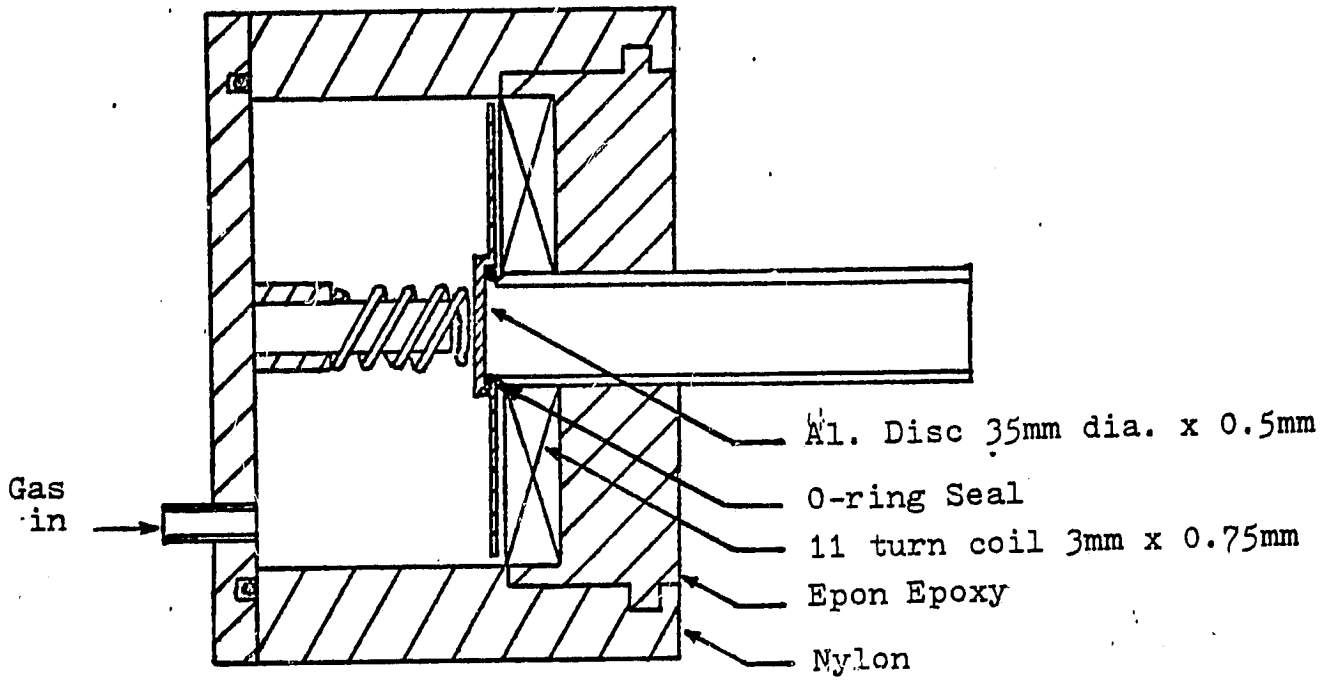

Figure 6.16. Sketch of fast gas value.

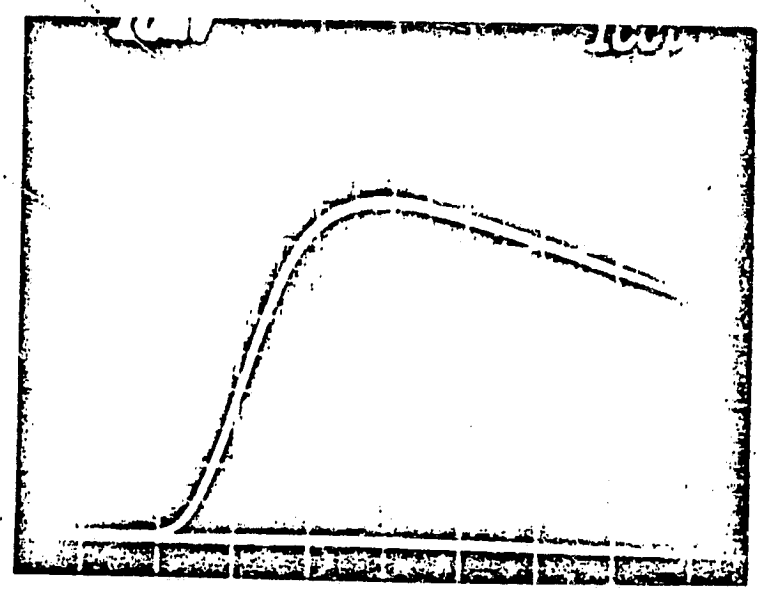

Figure 6.17. Pressure transient for above value 15cm away from nozzle.

References

1. Baldwin, D. E.,"End Loss Processes from Mirror Machines," *Rev. of Mod. Phys.*. 49, (1977), 317-339.

2. Baldwin, D. E. and Logan, B. G.,"Improved Tandem Mirror Reactor," *Phys. Rev. Lett.*. 43, 18 (1979).

3. Baldwin, D. E., "Physics Overview," *Physics Basis for MFTF-B*, Baldwin, *et al.*, eds.No. UCID-18496-Part I, (1980).

4. Bernstein, I. and Baxter,"Relativistic Theory of Electron Cyclotron Resonance Heating," *Phys. of Fluids.* 24, (1981), 108-126.

5. Carlson *et al.*,*Tandem Mirror Reactor with Thermal Barriers*, UCRL-52836, (1979).

6. Coensgen, F. H. *et al.*,"Multistage Magnetic Compression of Highly Ionized Plasma," *Phys. Fluids.* 2, (1959), 350.

7. Cohen, B.I., ed., *Status of Mirror Fusion Research*, No. UCAR-10049-80, (1980).

8. Coppi, B. *et al.*,"Slide Away Distributions and Relevant Collective Modes in High-Temperature Plasmas," *Nuc. Fusion.* 16, (1976), 2.

9. Dandle, R. A. *et al.*,"Off-resonance effects on electrons in mirror-contained plasmas," *Nuclear Fusion.* 11, (1971), 411-423.

10. EBT, *EBT Ring Physics*, Workshop proceedings, Oak Ridge, (1977).

11. Eldridge, O. *et al.*,*Electron Cyclotron Resonance Heating in Tokamaks*, ORNL-TM-6052, (1977).

12. Fessenden, T. J.,*Pulsed Electron-Cyclotron Resonance Discharge Experiment*, M.I.T.-R.L.E. Report 442, (1966).

13. Gerver, M. J.,*Electron Landau Damping of Loss-Cone Instabilities in a Mirror Reactor Regime*, M.I.T.-PFC, Sherwood Meeting, (1980).

14. Haste, G. R. and Lazor, N. H.,"Axial Distribution for a Hot Electron Plasma," *Physics of Fluids.* 16, (1973), 683.

15. Ikegami, H. *et al.*,"Generation of Energetic Electrons by Electron Cyclotron Heatingin a Magnetic Mirror Field," *Nuclear Fusion.* 13, (1973), 351-361.

16. Ikegami, H. and Dandle, R. A.,*Electron cyclotron heating for Bumpy Torus.* IPPJ-343, Nagoya, (1978).

17. Ioffe, M. S. *et al.*,"Magentic Mirror Confinement of a Plasma," *Sov. Phys., JETP.* 21, (1965), 40.

18. Ioffe, M. S. *et al.*,"Stabilization of Cone-Instability of A collisional Plasma in a Mirror Trap," *Soviet Phys. JETP.* 40, (1975), 1064.

19. Kanaev, B. I.,"Stabilization of drift loss-cone instability (DCI) by addition of cold ions," *Nuc. Fusion.* 19, (1979), 347.

20. Kennel, C. F. and Engelman, F.,"Velocity Space Diffusion from Weak Plasma Turbulence in a Magnetic Field," *Phys. of Fluids.* 9, (1966), 2377.

21. Kesner, J.,"Axisymmetric Sloshing-Ion Tandem Mirror Plugs," *Nuc. Fusion.* 20, (1980), 557-562.

22. Klinkowstein, R. E. and Smullin, L. D.,"Suppression of $\omega_c i$ instability in a mirror-confined plasma by injection of an electron beam," *Phys. Rev. Lett.*, 40, (1978), 771-773.

23. Lieberman, M. A. and Lichtenberg, A. J.,"Theory of Electron Cyclotron Resonance Heating-II Long Time and Stochastic Effects," *Plasma Phys.*, 15, (1973), 125-150.

24. Lawrence Livermore Laboratories, unpublished Nexsen, W. E. *et al.*,*Titanium Washer Stack Plasma Injectors,* (1977).

25. Mauel, M. E.,*Hot Electron Stabilization of DCLC with Electron Cyclotron Heating,* M.I.T. PRR-11/79, (1979).

26. Mauel, M. E. *et al.*,*Electron Cyclotron Heating of the Constance II Mirror Confined Plasma,* M.I.T., PRR-80/25, (1980).

27. Mauel, M. E.,*Discussion of Neutral Particle Effects and Power Balance in the Constance Mirror Experiment,* PRR 80/5, (1980).

28. Mauel, M. E.,*Theory of Electron Cyclotron Heating in the Constance II Experiment,* M.I.T., PFC-RR-81-2, (1981).

29. MFTF-B, *Physics Basis for MFTF-B,* Baldwin,*et al.*, eds.No. UCID-18496-I, (1980).

30. Moir *et al.*,*Preliminary Design Study of the Tandem Mirror Reactor,* UCRL-52302, (1977).

31. Nevins, W. M.,"Microstability of Thermal Barrier in Tandem Mirrors," *Bull. Amer. Phys. Soc.*, 25, (1980), 920.

32. Nezlin, M. V. and Solntsev, A. M.,"Unstable Plasma Beam," *Sov. Phys., JETP,* 21, (1965), 826.

33. Osher, J. E.,*Plasma Target Output from a Magnetically Augmented, Gas-Injected, Washer-Stack Plasma Gun,* UCRL-84480, (preprint, 1980).

34. Pearlstein, L. D., Smith, G. R. and Nevins, W. M., "Loss-Cone Instability," *Physics Basis for MFTF-B,* Baldwin, *et al.*, eds.No. UCID-18496-Part II, (1980).

35. Porkolab, M.,*Electron Cyclotron Resonance Heating of Tandme Mirrors,* UCRL-2-2634, (1978).

36. Porkolab, M. *et al.*,*Electron Cyclotron Resonanc Heating of Plasmas in Tandem Mirrors,* UCRL-84345, REv. 2, Lawrence Livermore Laboratory, (To be published).

37. Ray, J. A., Barrett, C. F. *et al.*,"Absolute Measurement of Low Energy H° Fluxes by a Secondary Emission Detector," *J. Appl. Phys.*, 50, (1979), 10.

38. Rose, D. J., ed., *Plasmas and Controlled Fusion,* M.I.T. Press, Cambridge, Mass, (1961).

39. Rudakov, L. I. and Tsytovich, V. N.,"Strong Langmuir Turbulence," *Physics Reports,* 40, (1978), 2.

40. Rymer, J. P.,, S.M.thesis, M.I.T., (1980).

41. Smatlak, O. *et al.*,"ECRH in Phaedrus," *Bull. of Amer. Phys. Soc.*, 25,, 860.

42. Stallard, B. W. and Hooper, E. B., Jr.,"Heating by ECRH in TMX-Upgrade," *Bull. of Amer. Phys. Soc.*, 25, (1980), 954.

43. Thornhill, S. G. and Haar, D.,"Langmuir Turbulence and Modulational Instability," *Physics Report,* 43, (1978), 44.

44. TMX Group, "Summary of Initial TMX Results," *Physics Basis For MFTF-B,* Baldwin, *et al.*, eds.No. UCID 18496-Part I, (1980).

45. TARA,*Construction of TARA Tandem Mirror Facility,* PFC Project Proposal, (1980).

46. Vibrans, G. E.,*Calculation of the Surface Temperature of a Solid Under Electron Bombardment,* Lincoln Laboratory Technical Report No. 268, (1962).

END

DATE FILMED

09/29/81